

*Rational Design of Mixed-Metal Oxides for Chemical
Looping Combustion of Coal via Experimental and
Computational Studies*

Amit Mishra*

Nathan Galinsky

Arya Shafiefarhood

Erik Santiso (co-PI)

Fanxing Li (PI)

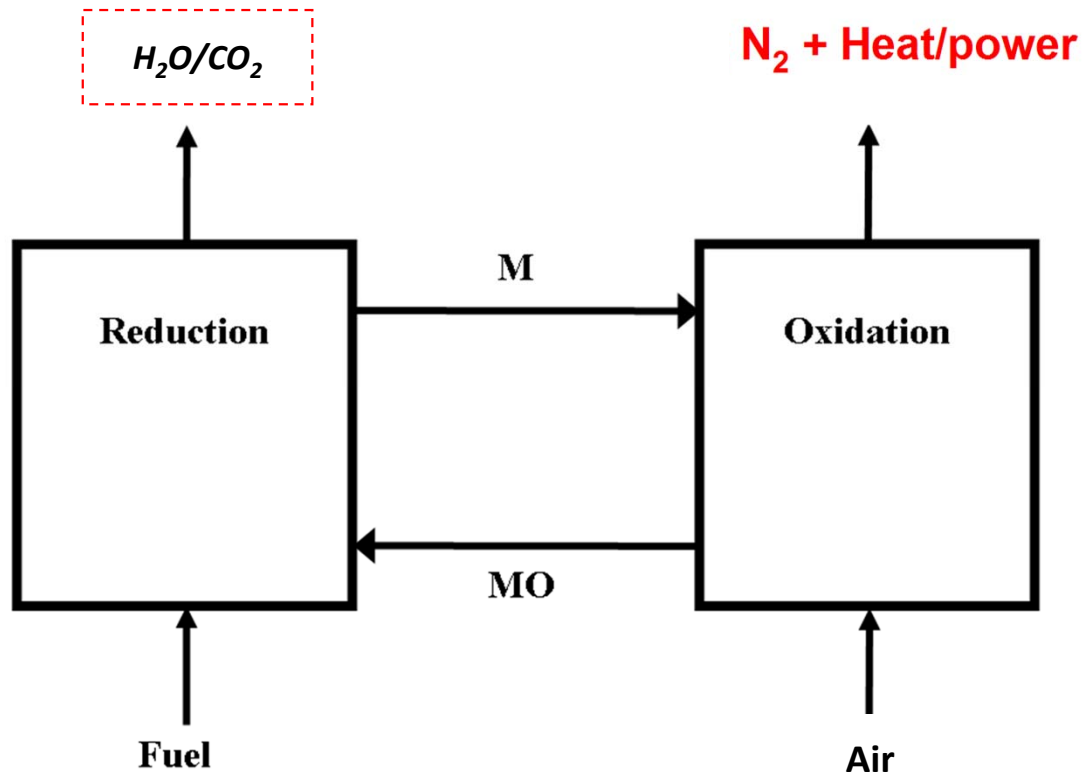


04/19/2016

Outline

- Background
- Selection criteria for commercially viable oxygen carriers
- Computational investigation of $\text{Ca}_x\text{A}_{1-x}\text{Mn}_y\text{B}_{1-y}\text{O}_3$ based oxygen carriers
- Experimental findings
- Conclusions

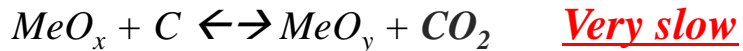
Carbonaceous Fuel Conversions via Chemical-Looping Combustion



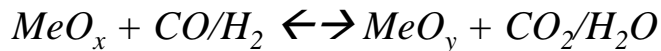
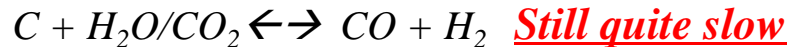
- 2-Step Redox Loop
- Product: Heat, Power
- Integrated CO₂ Capture

Chemical Looping Processes – Challenges and Opportunities for Coal Conversion

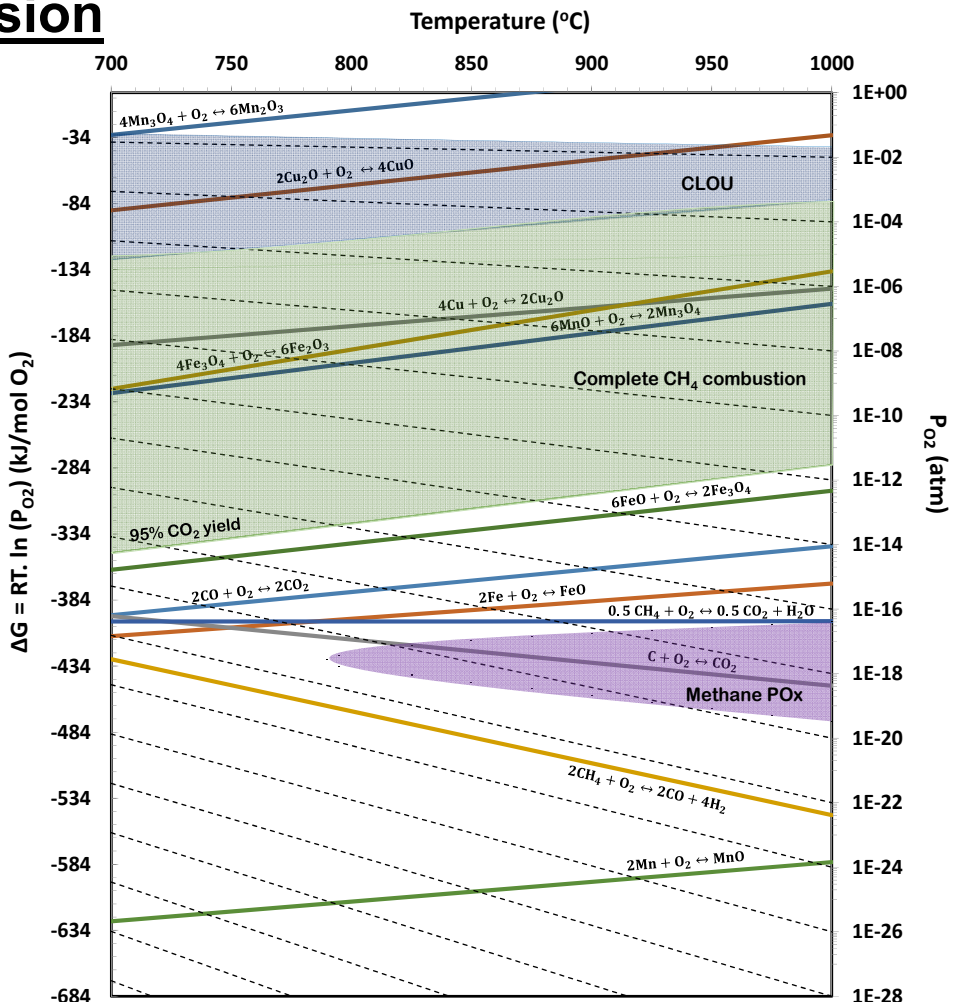
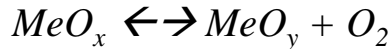
Challenge: Solid-solid reaction



Solution I: In-situ gasification of solid fuel

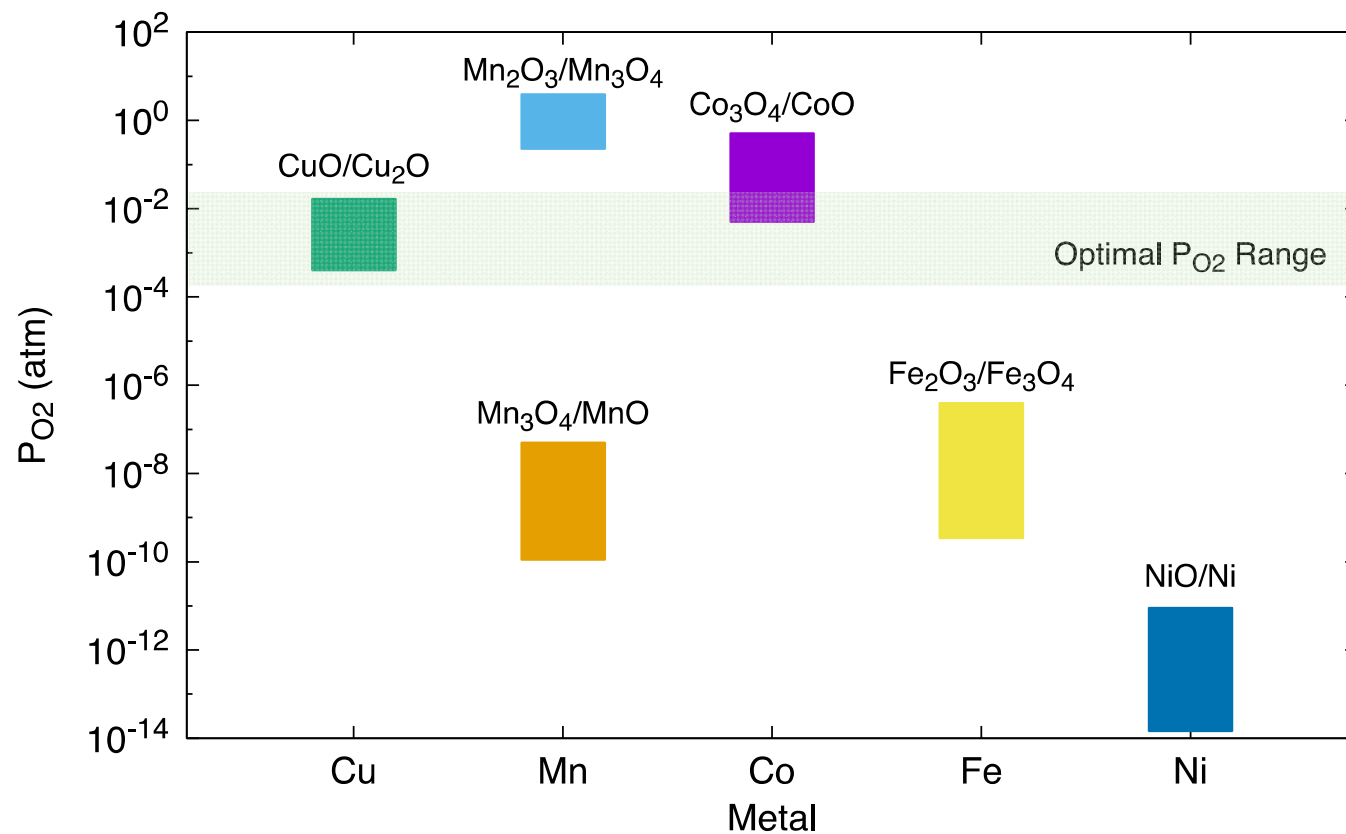


Solution II: Chemical Looping with Oxygen uncoupling



Chemical Looping with Oxygen Uncoupling (CLOU) is a promising approach for coal combustion

Oxygen Carrier Selections

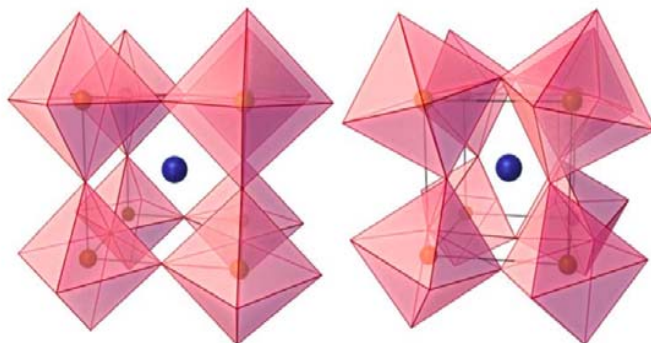


CuO is the only mono-metallic oxide exhibiting desirable CLOU properties. However, it is costly and has high tendency for sintering.

Material Selection – Rapidly Expanding Material Design Space

Oxygen carrier selections

- Iron
- Copper
- Manganese
- Nickel
- Cobalt
- Mixed first row transition metal oxides
- Perovskite materials



The periodic table is shown from period 1 to 7. A legend indicates that open circles represent A site atoms and filled circles represent B site atoms. The highlighted area covers the first seven columns (Groups 1-7), which correspond to the A and B sites in the perovskite structure.

	IA	IIA						0
1	H							
2	Li	Be						
3	Na	Mg	III A	VA	VA	VIA	VII A	
4	K	Ca	Sc	Ti	V	Cr	Mn	Fe
5	Rb	Sr	Y	Zr	Nb	Mo	Tc	Ru
6	Cs	Ba	La	Hf	Ta	W	Re	Os
7	Fr	Ra	Ac					
			Ce	Pr	Nd	Pm	Sm	Eu
			Th	Pa	U	Np	Pu	Am
								Cm
								Bk
								Cf
								Es
								Fm
								Md
								No
								Lr

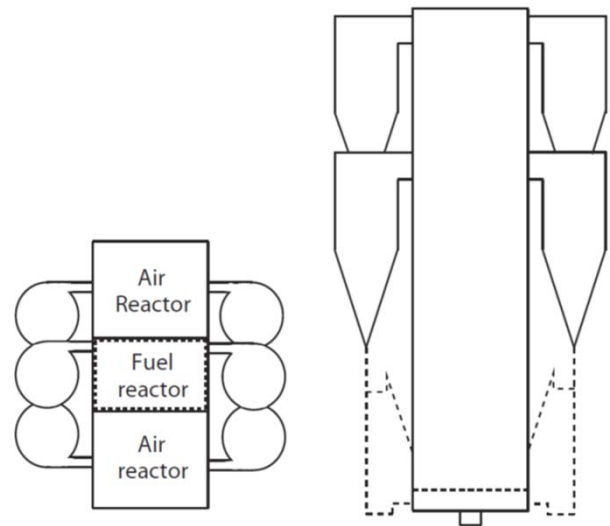
M. Rydén et al., 2nd International Conference on Chemical Looping, 2012
Structure and Properties of Perovskite Oxides, Tatsumi Ishihara

Outline

- Background
- Selection criteria for commercially viable oxygen carriers
- Computational investigation of $\text{Ca}_x\text{A}_{1-x}\text{Mn}_y\text{B}_{1-y}\text{O}_3$ based oxygen carriers
- Experimental findings
- Conclusions

Reactor Scale Up Considerations

Parameter	Literature	Scale-Up
Power	1.5 kW _{th}	1000 MW _{th}
Oxygen Carrier	CuO	CaMnO ₃
Solids Inventory (kg/MW_{th})	100-250	350
Solids Fraction	0.45	0.45
Density (kg/L)	4.6	2.5
Reactor Volume Inventory (L/MW_{th})	40-120	310
Reactor Dimensions	50mm x 200mm	7.3m x 7.3m
Linear Velocity (m/s) in the inlet	0.11	0.11
Linear Velocity (m/s) at the outlet	0.5	9
Assuming 100% conversion of coal		
Coal Heating Value (MJ/kg)	20-35	25.9
Coal Feed Rate (tonne/hr)	0.00011	139.1
Solids Circulation Rate (tonne/hr)	0.0042	35,000



1. Abad, A. et al. Demonstration of chemical-looping with oxygen uncoupling (CLOU) process in a 1.5kWth continuously operating unit using a Cu-based oxygen-carrier. *Int. J. Greenh. Gas Control* **6**, 189–200 (2012).

2. García-Labiano, F., de Diego, L. F., Adánez, J., Abad, A. & Gayán, P. Reduction and Oxidation Kinetics of a Copper-Based Oxygen Carrier Prepared by Impregnation for Chemical-Looping Combustion. *Ind. Eng. Chem. Res.* **43**, 8168–8177 (2004).

3. Eyring, E. M. et al. Chemical Looping with Copper Oxide as Carrier and Coal as Fuel. *Oil Gas Sci. Technol. – Rev. D’IFP Energ. Nouv.* **66**, 209–221 (2011).

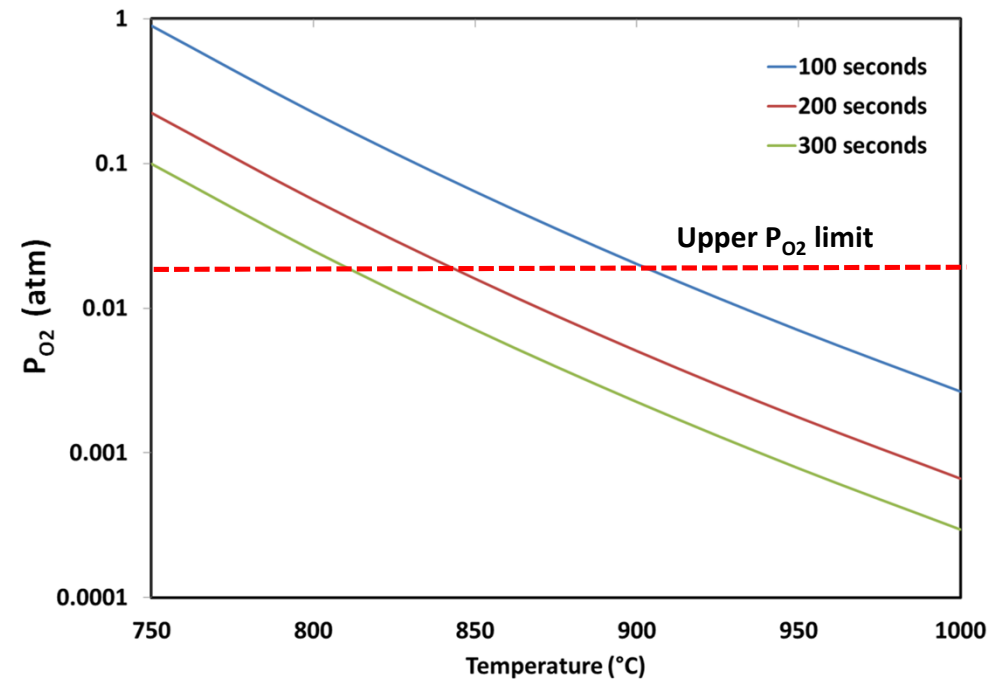
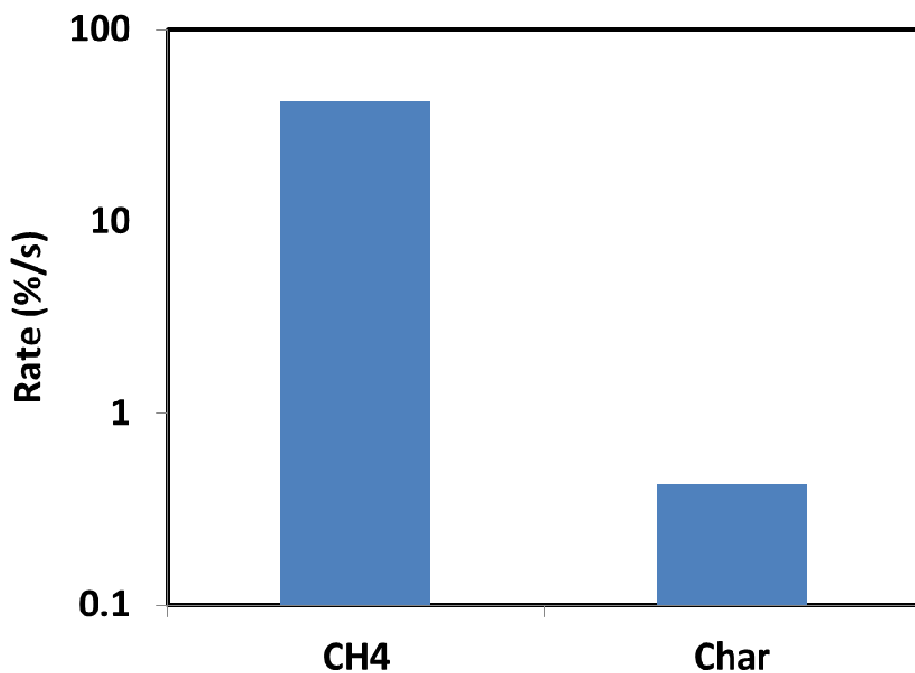
4. Markström, P., Linderholm, C. & Lyngfelt, A. Chemical-looping combustion of solid fuels – Design and operation of a 100kW unit with bituminous coal. *Int. J. Greenh. Gas Control* **15**, 150–162 (2013).

5. Berguerand, N. & Lyngfelt, A. Design and operation of a 10kWth chemical-looping combustor for solid fuels – Testing with South African coal. *Fuel* **87**, 2713–2726 (2008).

6. Sahir, A. H., Sohn, H. Y., Leion, H. & Lighty, J. S. Rate Analysis of Chemical-Looping with Oxygen Uncoupling (CLOU) for Solid Fuels. *Energy Fuels* **26**, 4395–4404 (2012).

7. Anders Lyngfelt and Bo Leckner. A 1000 MWth boiler for chemical-looping combustion of solid fuels – discussion of design and costs. *Applied Energy* **157**, 475-487 (2015)

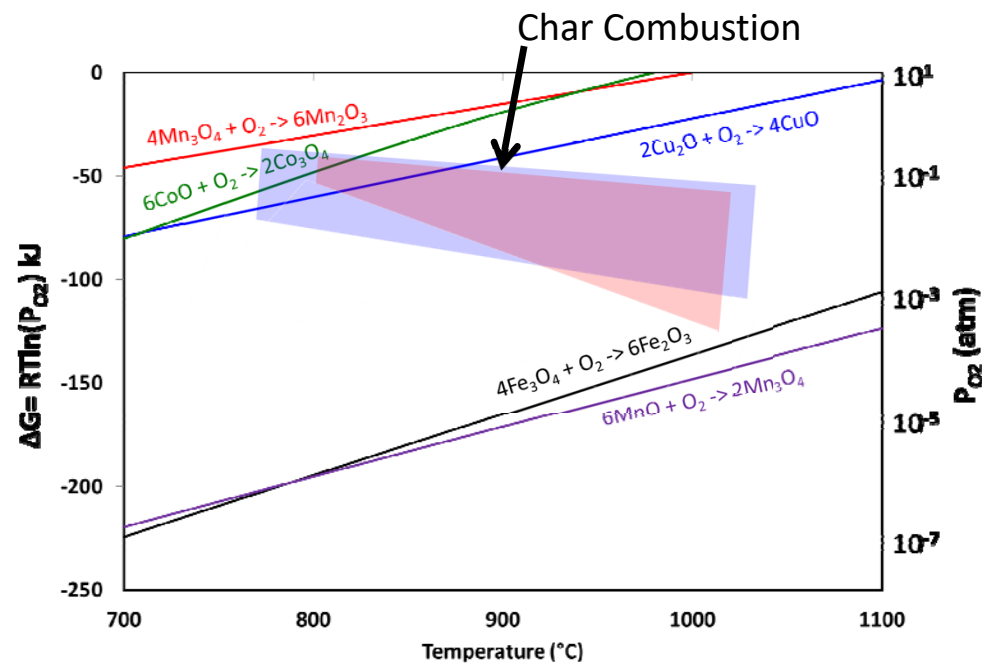
Kinetics- Gas vs Solids



Over two order of magnitude faster kinetics for CH₄ when compared to bituminous char. A “critical” P_{O_2} range can be determined by char combustion kinetics.

Determination of Critical P_{O₂} Range

Residence time of coal (s)		200
Parameters:	Experimental	Literature
Model	Arrhenius	Shrinking Core
Coal Type:	Illinois #6 (bituminous)	Pocahontas (bituminous)
Order of reaction (n)	0.92	0.5-1 (0.5 used)
Activation Energy (kJ/mol)	28	126
Pre-exponential factor (A)	414.3 atm ^{-0.92} s ⁻¹	930 g•cm ⁻² atm ^{-0.5} s ⁻¹
Temperature (°C)	950	950
Equilibrium P _{O₂} (atm)	0.013	0.0032



1. Sahir, A. H., Sohn, H. Y., Leion, H. & Lighty, J. S. Rate Analysis of Chemical-Looping with Oxygen Uncoupling (CLOU) for Solid Fuels. *Energy Fuels* **26**, 4395–4404 (2012).

2. Tian, X., Su, M., Zhao, H., Kinetics of lignite char gasification and combustion in rich-CO₂ and/or lean-O₂ atmosphere: A similar condition in coal-derived CLOU processes. Proceedings of the Combustion Institute. (accepted)

Outline

- Background
- Selection criteria for commercially viable oxygen carriers
- Computational investigation of $\text{Ca}_x\text{A}_{1-x}\text{Mn}_y\text{B}_{1-y}\text{O}_3$ based oxygen carriers
- Experimental findings
- Conclusions

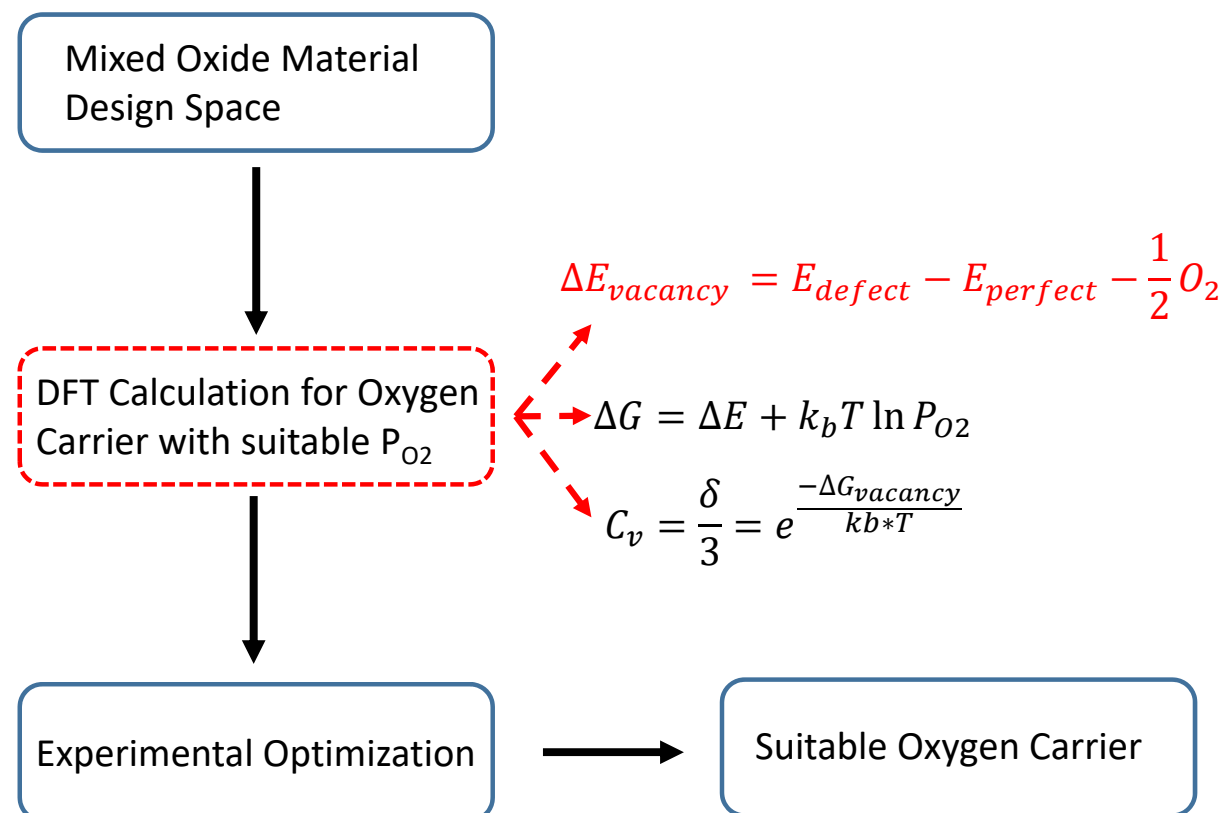
First Principles Approach Towards Screening/Elucidation of Oxygen Carriers

- Material Investigated:

- $\text{CaMnO}_{3-\delta}$
- $\text{CaMn}_{0.75}\text{Fe}_{0.25}\text{O}_{3-\delta}$
- $\text{Ca}_{0.75}\text{Sr}_{0.25}\text{MnO}_{3-\delta}$
- $\text{BaMnO}_{3-\delta}$

- Key Variables?

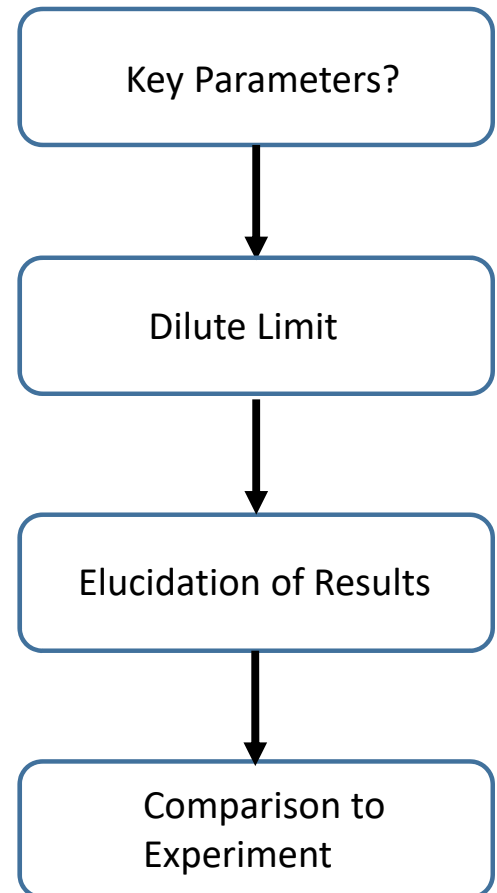
- Low energy spin configuration
- Hubbard U (PAW-PBE + U)
- Oxygen sites in doped structure
- Dilute Limit





Approach

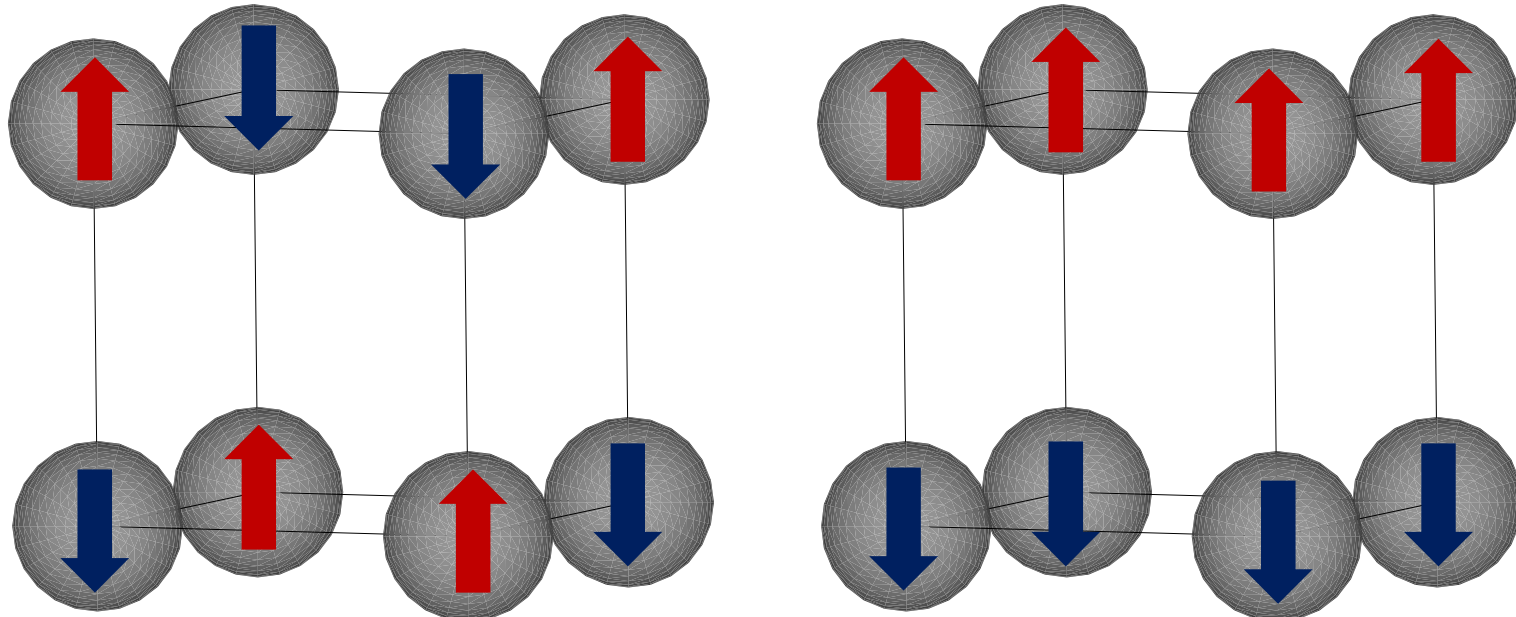
- Addressing key parameters
 - Effect of spin configuration
 - Effect of Hubbard U parameter
 - Determination of oxygen sites in doped structures
- Determination of Dilute of limit
- Elucidation of results
- Extension to experiments
- Possible improvements to method





Spin Configurations

G-Type Antiferromagnetic (GAF) A-Type Antiferromagnetic (AF)



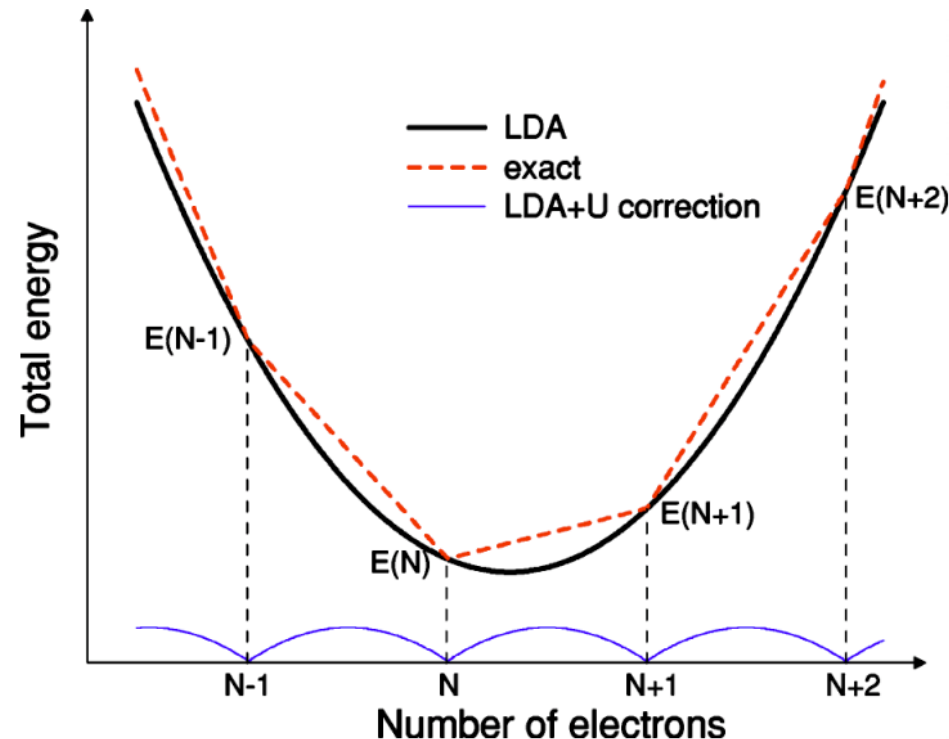
- Different spin orderings are possible and need to be considered



Improvement of DFT for correlated systems: Hubbard U

- Introduces a penalty for partial occupation of orbitals¹
- Methods for determining this:
 - Fitting to lattice parameters
 - Higher level of theory
 - Linear response method²
 - Energy of reduction³

$$E = E_{DFT} + \frac{U}{2} \sum_{I,\sigma} \sum_i \lambda_i^{I\sigma} (1 - \lambda_i^{I\sigma})$$



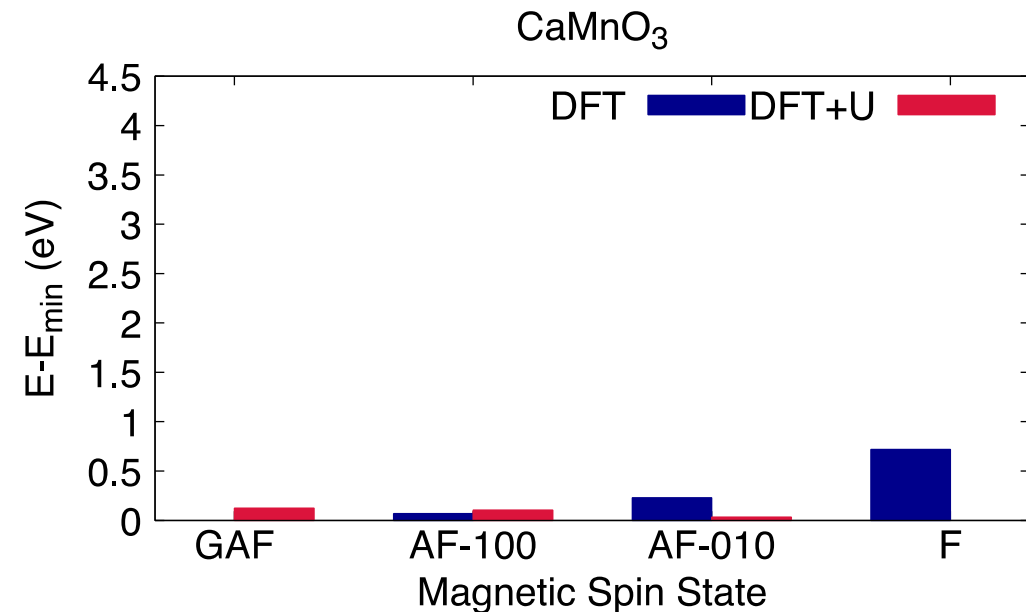
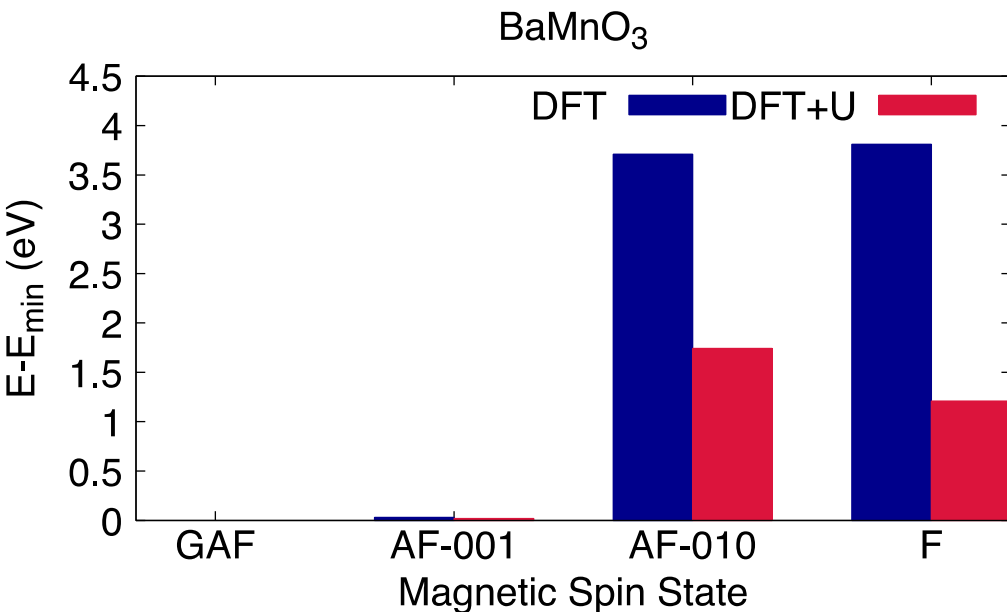
[1] S. L. Dudarev, G. A. Botton, S. Y. Savrasov, C. J. Humphreys and A. P. Sutton, *Phys. Rev. B*, 1998, **57**, 1505–1509.

[2] M. Cococcioni and S. de Gironcoli, *Phys. Rev. B*, 2005, **71**, 035105.

[3] L. Wang, T. Maxisch and G. Ceder, *Phys. Rev. B*, 2006, **73**, 195107



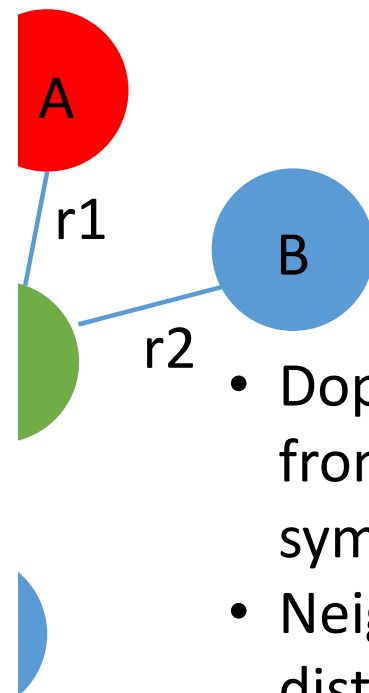
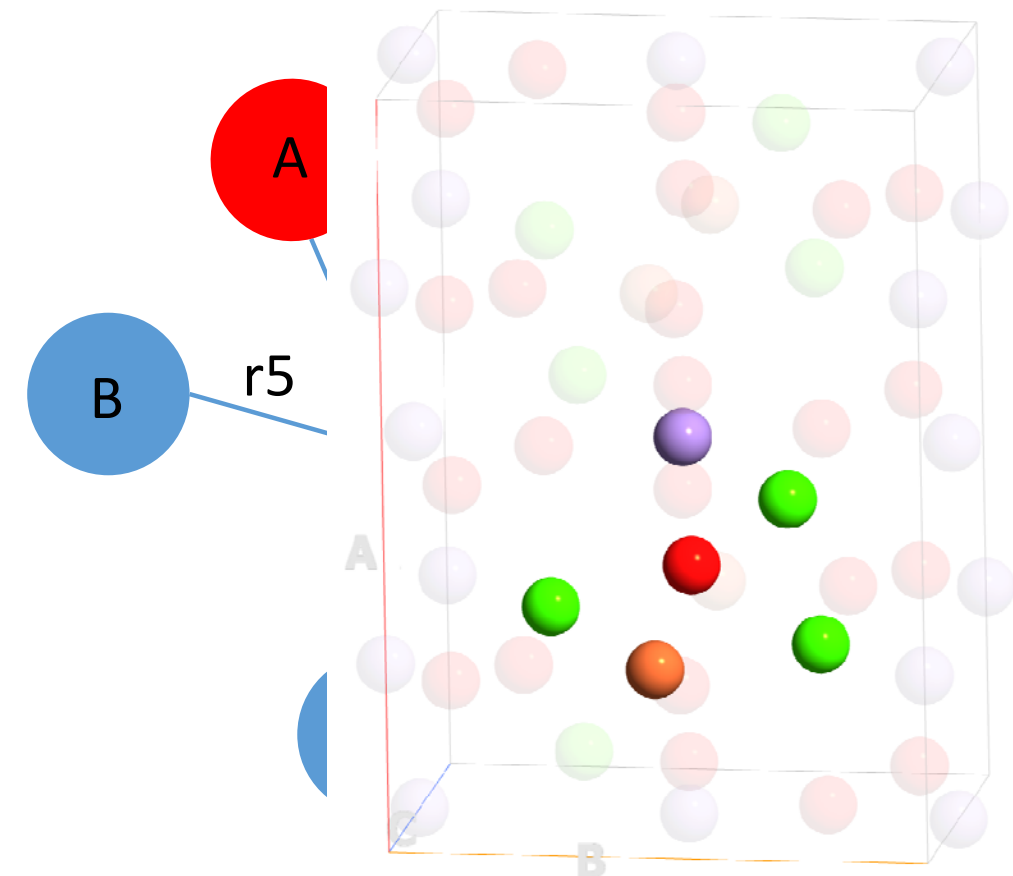
Stable Magnetic Configuration



- G-type antiferromagnetic spin ordering is predicted for BaMnO_3 using DFT and DFT+U
- DFT and DFT+U predicts different ordering for CaMnO_3
 - DFT: g-type antiferromagnetic, used for future DFT calculations
 - DFT+U: ferromagnetic, used for future DFT+U calculations
- Calculated results matches well with lattice parameters obtained from XRD/Rietveld Refinement



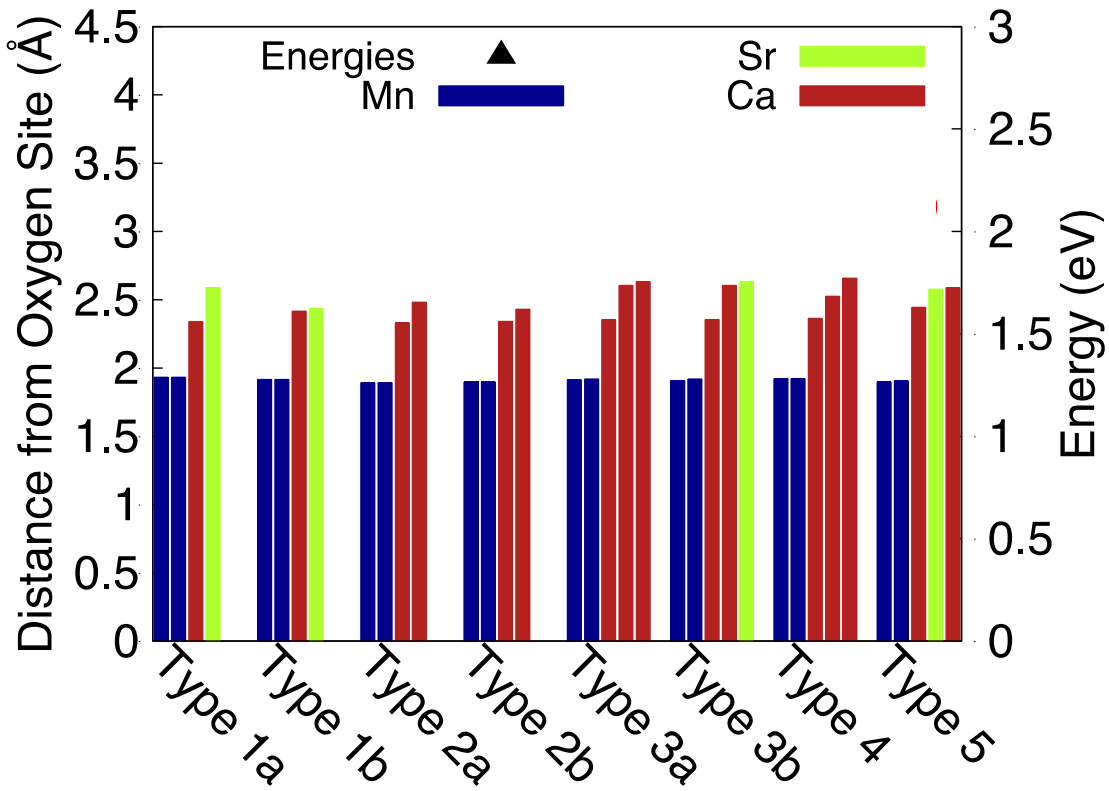
Determination of Unique Oxygen Sites in Doped Structures by Cation Neighbors



- Doping will distort structure from perfect $\text{CaMnO}_{3-\delta}$ symmetry
- Neighboring cations and distance from oxygen will determine unique oxygen
- Either 4 or 5 fold coordinated

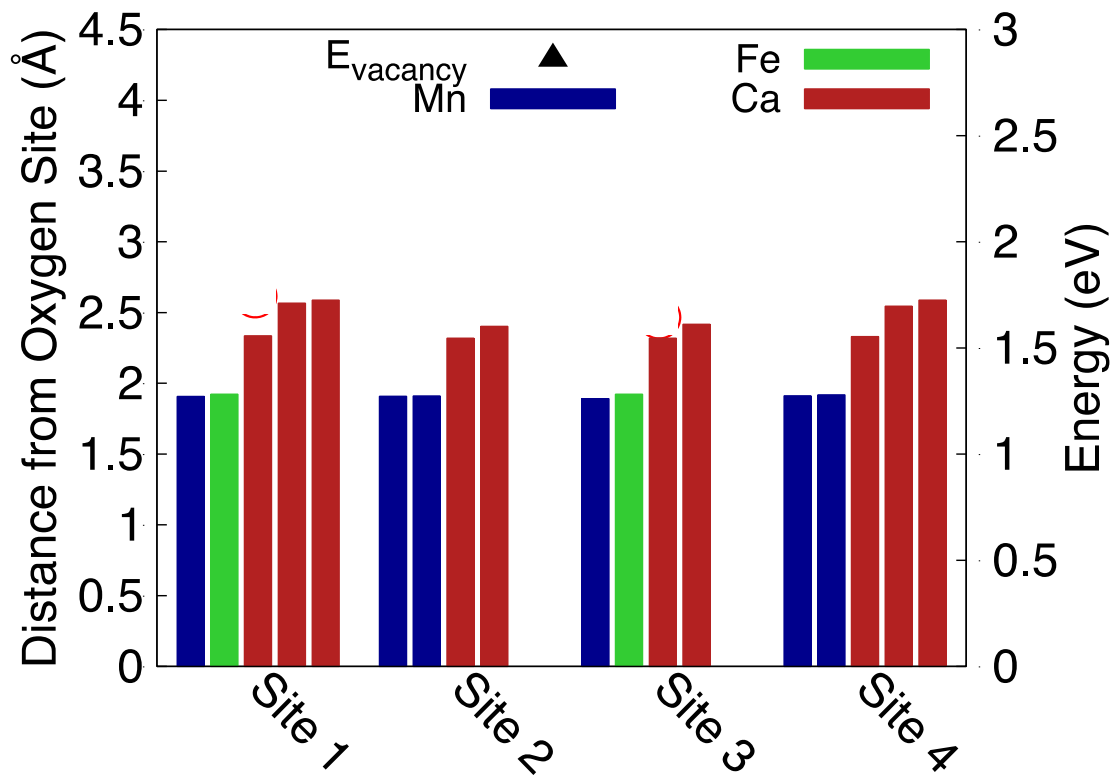


Unique Local Environments in $\text{Ca}_{0.75}\text{Sr}_{0.25}\text{MnO}_{3-\delta}$



- Sr doping induces twice as many oxygen sites as Fe doping
- Expected to be due to the size of Sr
- Type 2a, 5 have lowest energy of vacancy formation
- Results shown use DFT

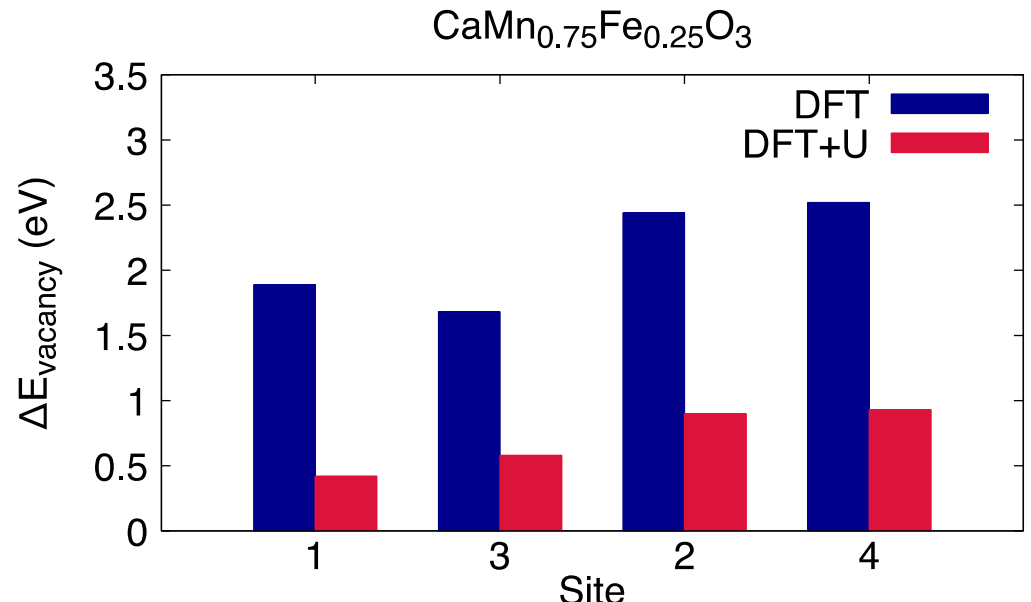
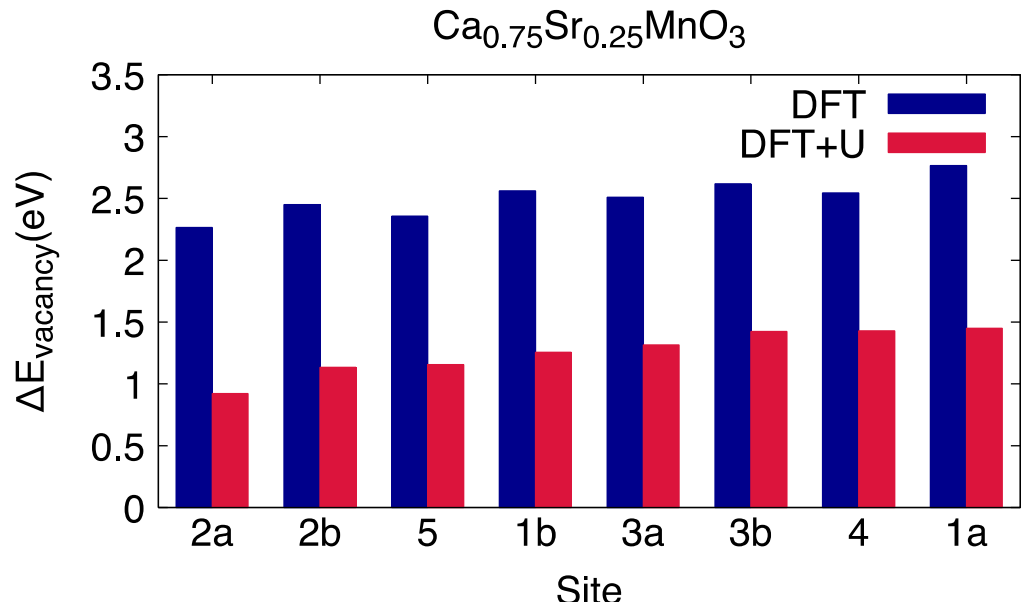
Unique Local Environments in $\text{CaMn}_{0.75}\text{Fe}_{0.25}\text{O}_{3-\delta}$



- Unique oxygen sites were determined according to nearest neighbors in 40 atom supercell
- Type 1 and Type 3 have lowest energy
- Results shown use DFT



Effect of Hubbard U on Energies

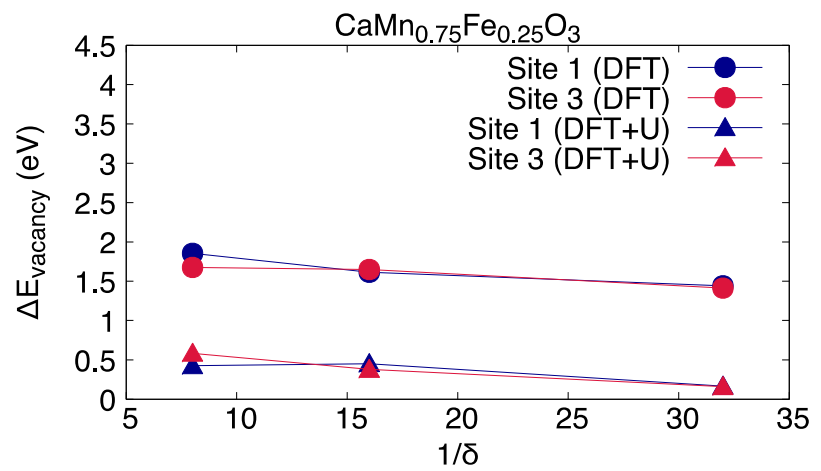
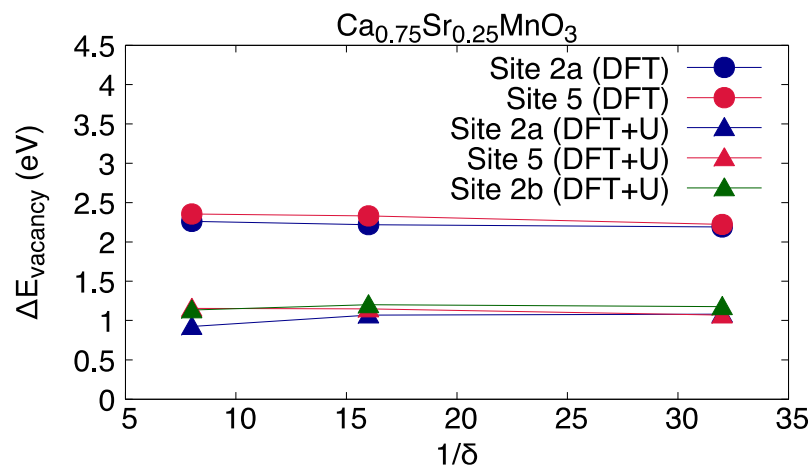
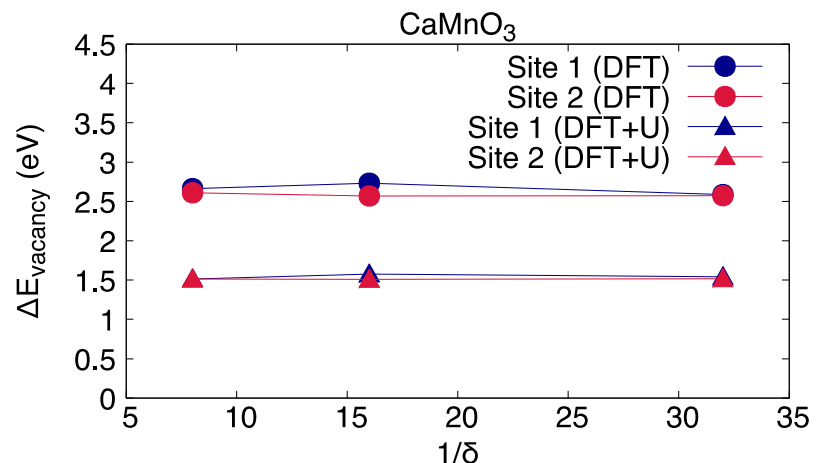
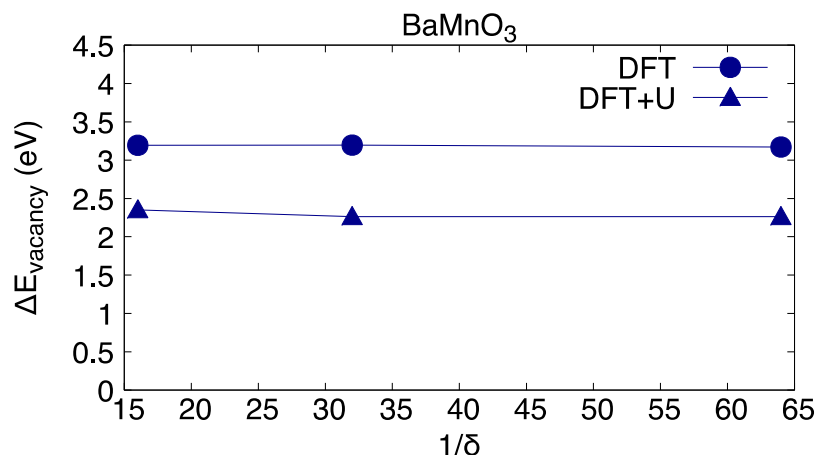


- For $\text{CaMn}_{0.75}\text{Fe}_{0.25}\text{O}_3$, DFT and DFT+U predicts the same site (1 and 3)
- For $\text{Ca}_{0.75}\text{Sr}_{0.25}\text{MnO}_3$, DFT predicts 2a and 5 and DFT+U predicts 2a, 2b, and 5

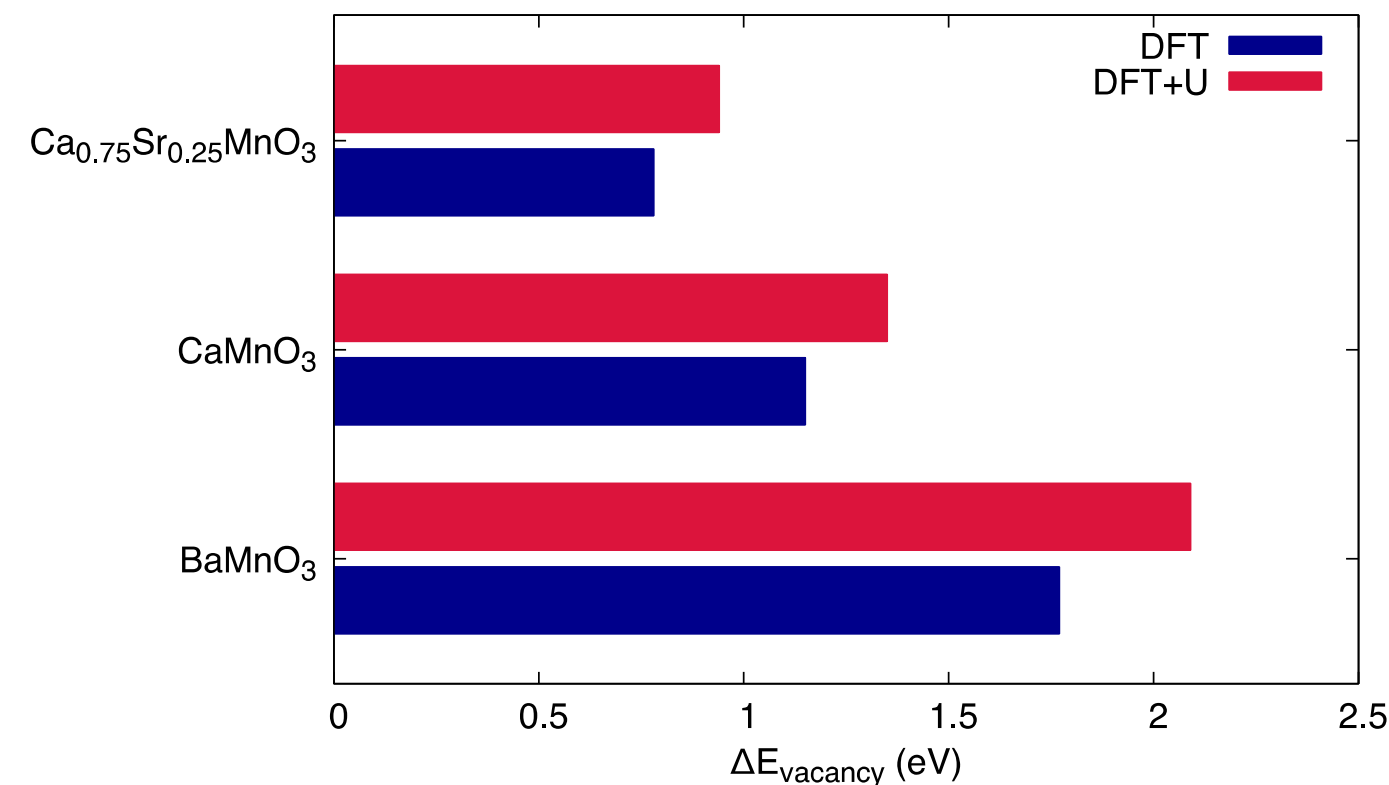


NC STATE UNIVERSITY

Dilute Limit for Materials



Ranking by $\Delta E_{\text{vacancy}}$

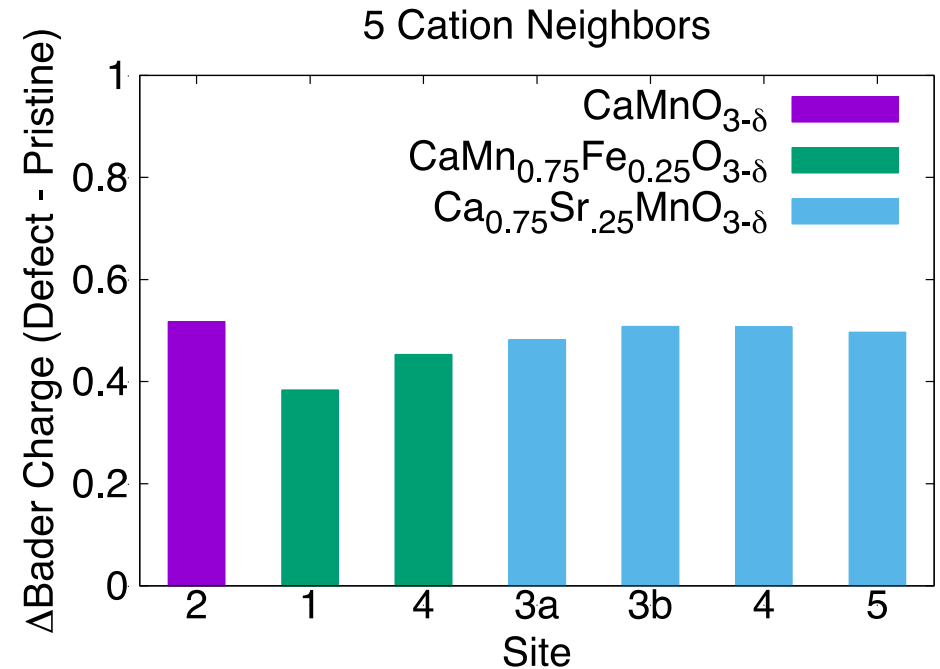
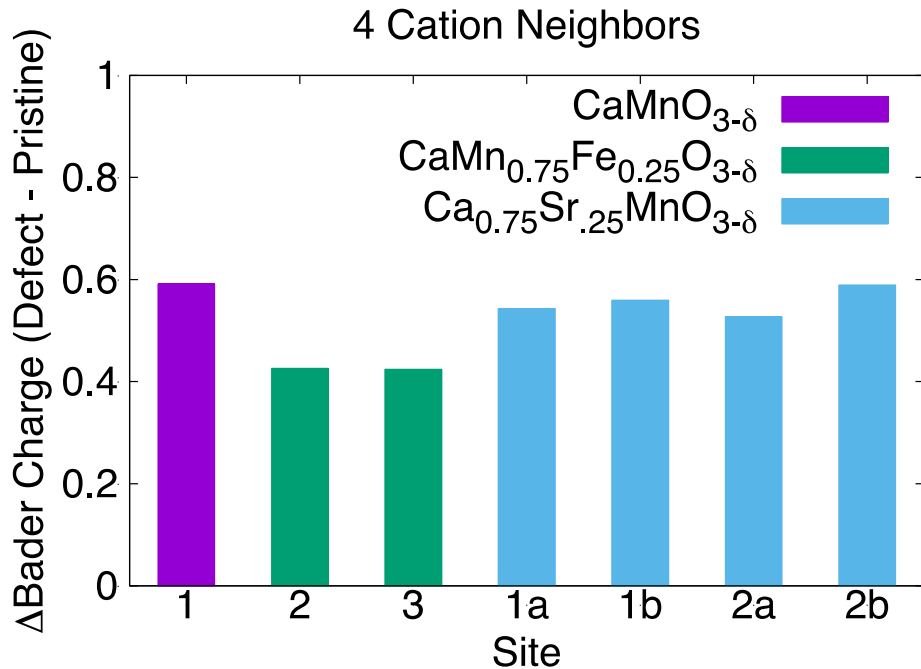


Predicted Oxygen
Donation:

- 1) $\text{CaMn}_{0.75}\text{Fe}_{0.25}\text{O}_3$
- 2) $\text{Ca}_{0.75}\text{Sr}_{0.25}\text{MnO}_3$
- 3) CaMnO_3
- 4) BaMnO_3

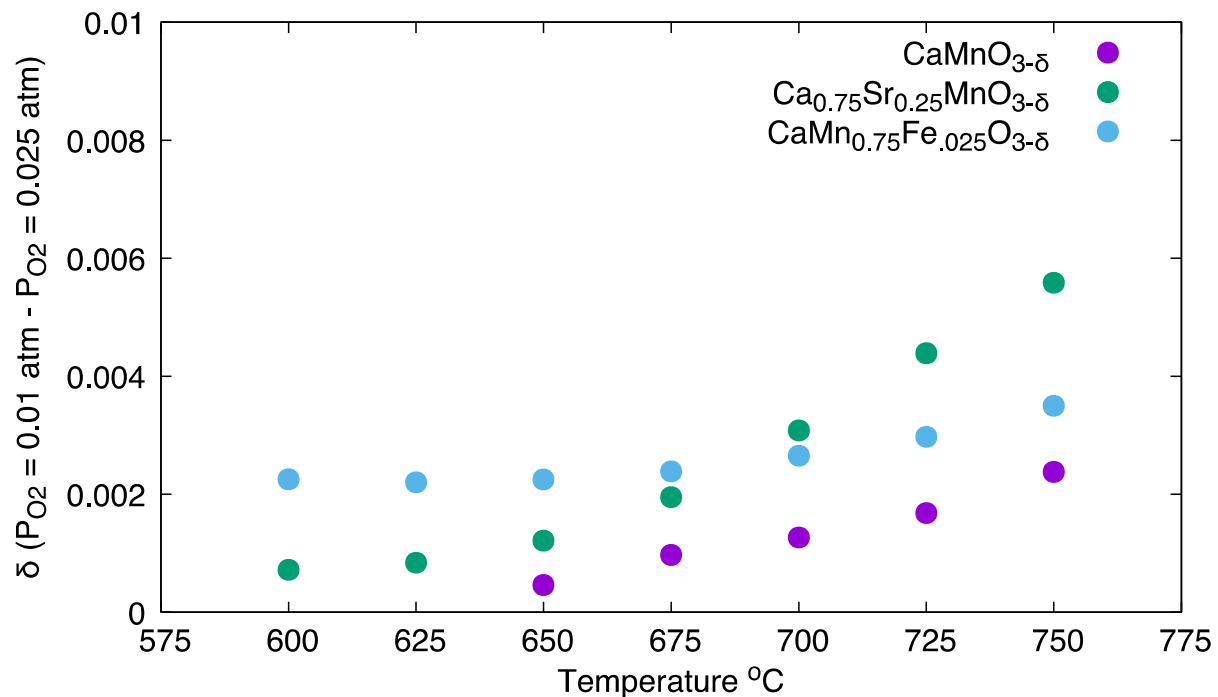


Degree of Delocalization



- Degree of delocalization is $\text{CaMn}_{0.75}\text{Fe}_{0.25}\text{O}_{3-\delta} > \text{Ca}_{0.75}\text{Sr}_{0.25}\text{MnO}_{3-\delta} > \text{CaMnO}_{3-\delta}$
- Inverse relationship with energy of vacancy creation

Experimental Results on Oxygen Donation



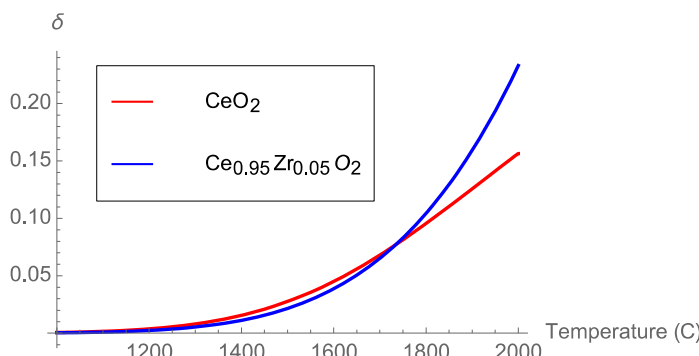
- Ranking of oxygen donation corresponds well with DFT results
- Beyond 675°C, oxygen donation from CSM surpasses CMF, due to entropy contribution

Entropy Contribution

$$Eq. 1: \frac{1}{2} \ln \left(\frac{P_{O_2}}{P^o} \right) = \frac{-\Delta h_\delta^o}{RT} + \frac{\Delta s_\delta^o}{R} |_{\delta=constant}$$

$$Eq. 2 \Delta s_\delta^o = \Delta s_{th} + \frac{1}{\delta_m} R (\ln(\delta_m - \delta) - \ln(\delta))$$

$$Eq. 3: \delta = \frac{\delta_m \left[\left(\frac{P_{O_2}}{P^o} \right)^{-0.5} e^{\left(\frac{\Delta s_{th}}{R} \right)} e^{\left(\frac{-\Delta h_\delta^o}{RT} \right)} \right]^{\delta_m}}{1 + \left[\left(\frac{P_{O_2}}{P^o} \right)^{-0.5} e^{\left(\frac{\Delta s_{th}}{R} \right)} e^{\left(\frac{-\Delta h_\delta^o}{RT} \right)} \right]^{\delta_m}}$$



Methods for Finding Δh_δ^o , Δs_{th} , δ_m

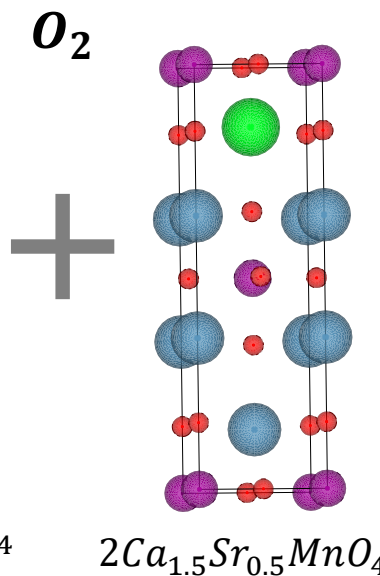
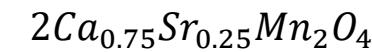
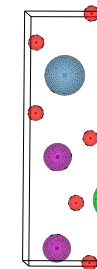
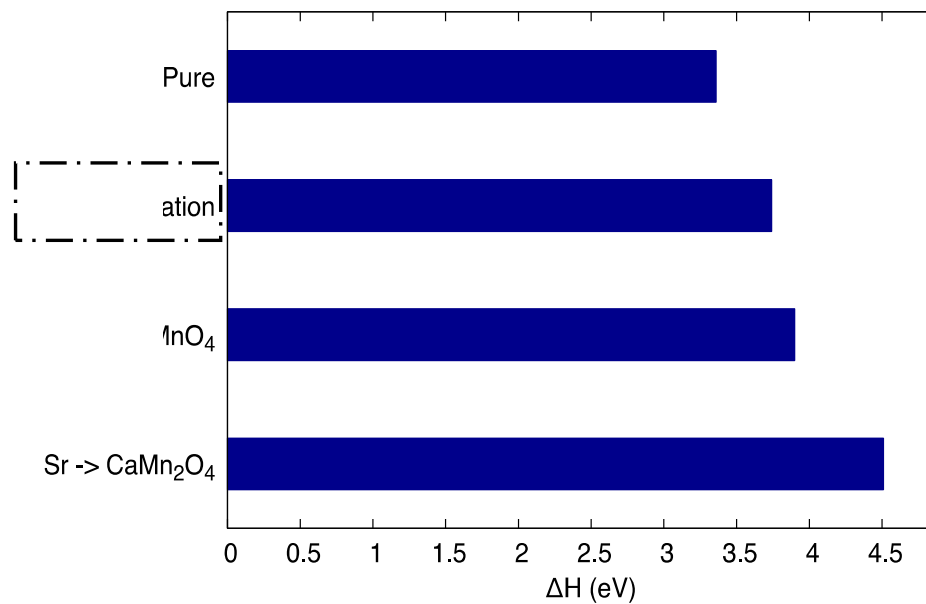
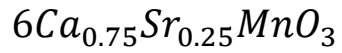
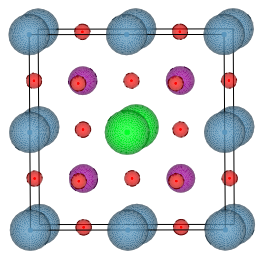
- DFT
 - $\Delta h_\delta^o = E_{vac}$
 - $\Delta s_{th} = \text{Phonon calculations, determine vibrational frequency}$
- Experimental
 - Thermogravimetric analysis and fit Eq. 1.
- $\delta_m = 0.5$ for perovskite

1. Bulfin, B. et al. Statistical thermodynamics of non-stoichiometric ceria and ceria zirconia solid solutions. *Phys. Chem. Chem. Phys.* **18**, 23147–23154 (2016).



NC STATE UNIVERSITY

Phase Segregation Inhibition by Sr

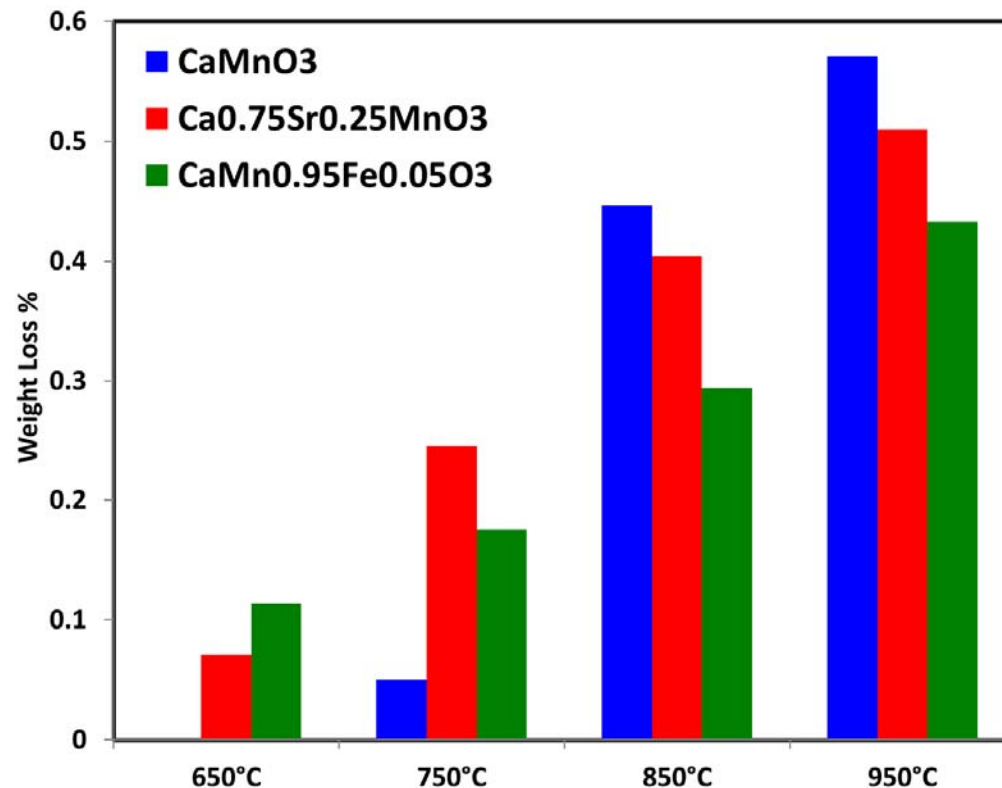


- $\text{Ca}_{0.75}\text{Sr}_{0.25}\text{MnO}_3$ is more stable than CaMnO_3 in all cases

Outline

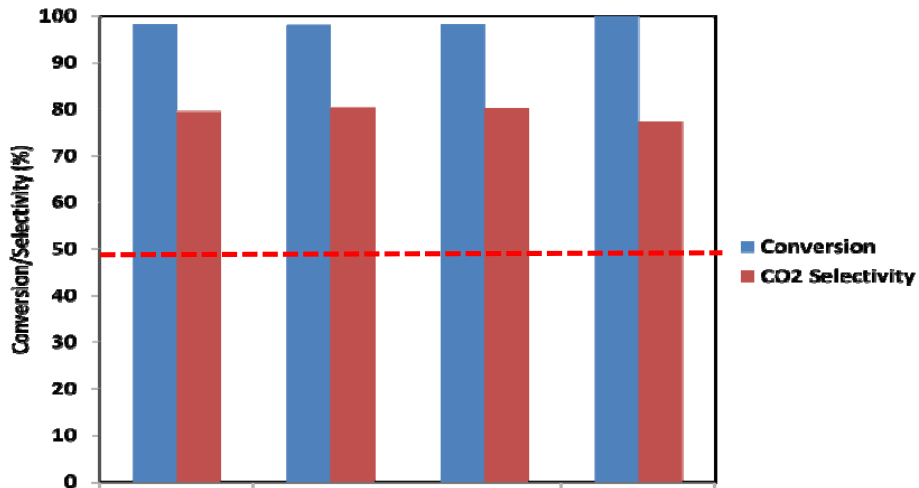
- Background
- Selection criteria for commercially viable oxygen carriers
- Computational investigation of $\text{Ca}_x\text{A}_{1-x}\text{Mn}_y\text{B}_{1-y}\text{O}_3$ based oxygen carriers
- **Experimental findings**
- Conclusions

CLOU Property Comparisons



Doping of the A- and B-site of CaMnO₃ allows for more low temperature oxygen desorption. CaMnO₃ does not observe much oxygen release below 800°C

Fluidized Bed Experiments



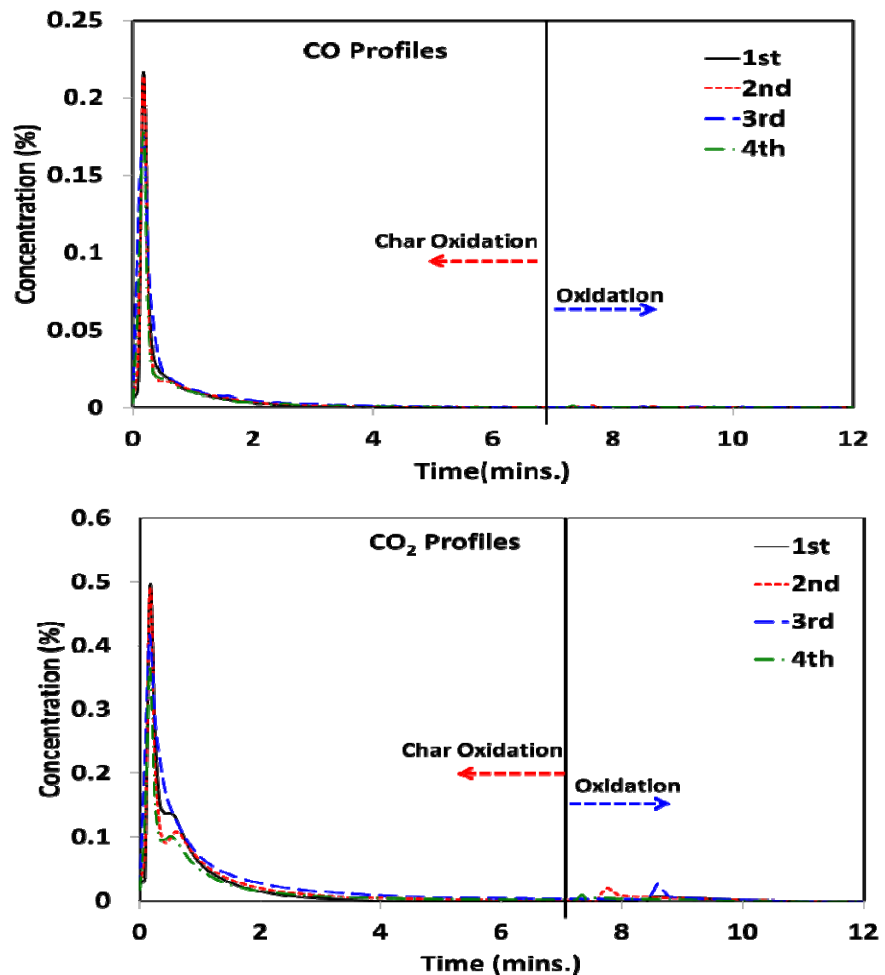
Char cycles after 20 hours operation in helium/10% O₂ redox mode (~60 cycles) and 10 other char cycles spread throughout the 20 hours of operation

Temperature: 850°C

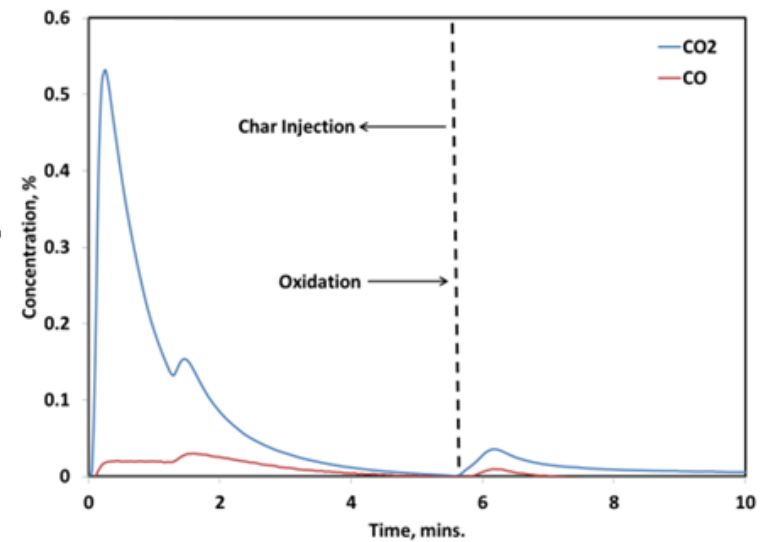
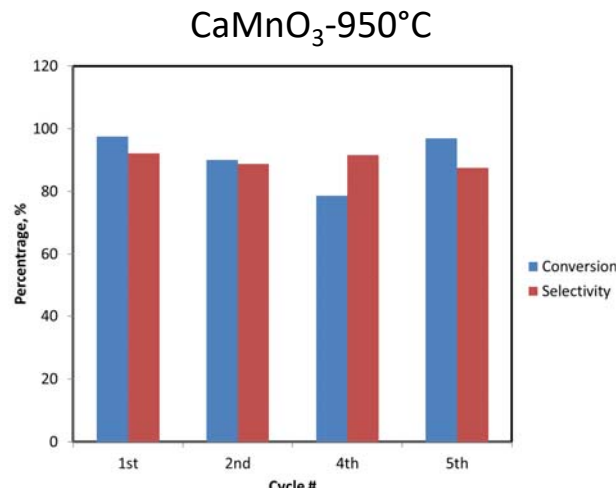
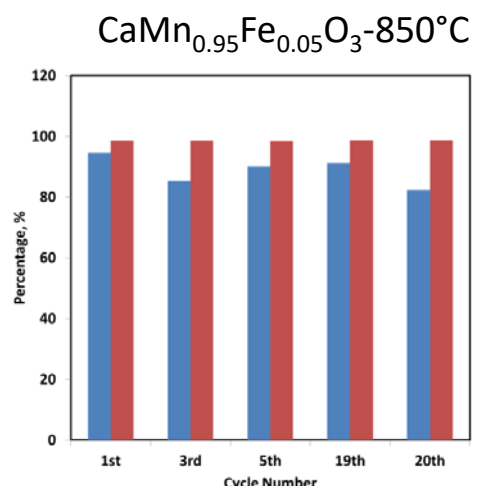
Fluidization velocity: 6 times of U_{mf}

Coal Used: Sea coal (bituminous)

Attrition rate: <0.02%/hour



Fluidized Bed-Experiments



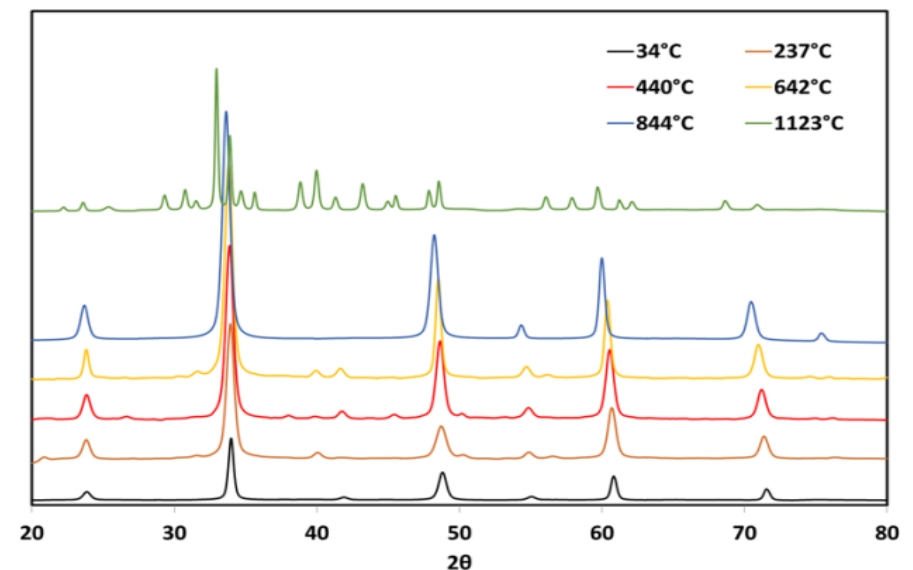
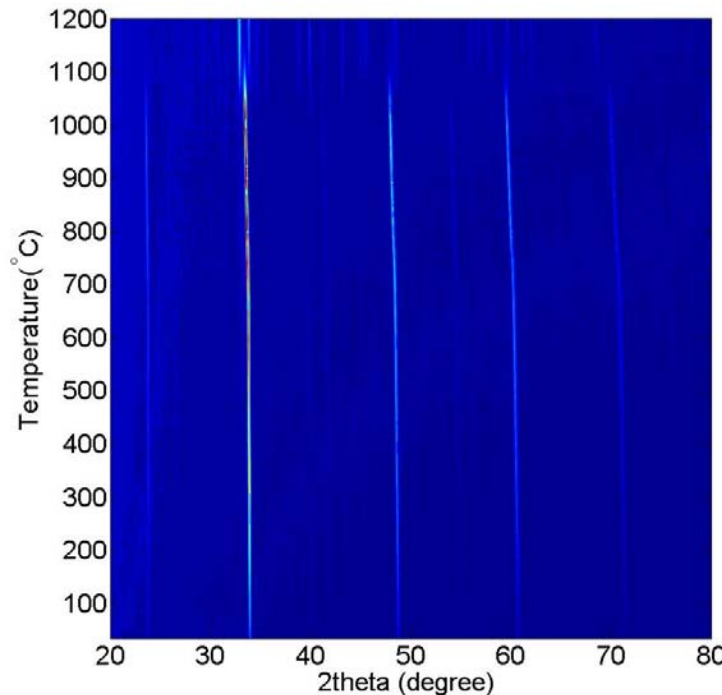
Fluidization velocity: 6 times of U_{mf}

Coal Used: Pittsburgh #8 coal (bituminous)

Attrition rate: <0.01 w.t.%/hour

Undoped CaMnO_3 was unable to achieve above 20% conversion at 850°C. Doped perovskites offer better low temperature conversion of coal char particles.

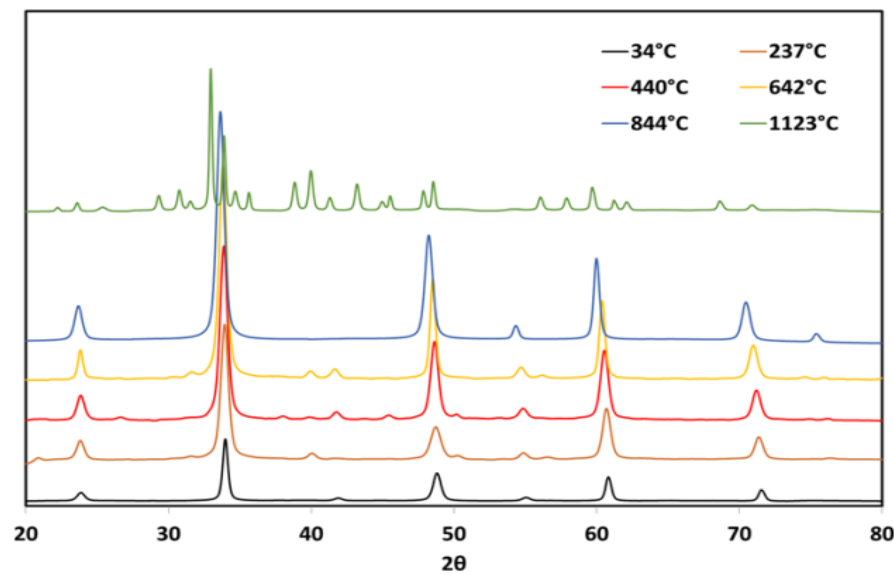
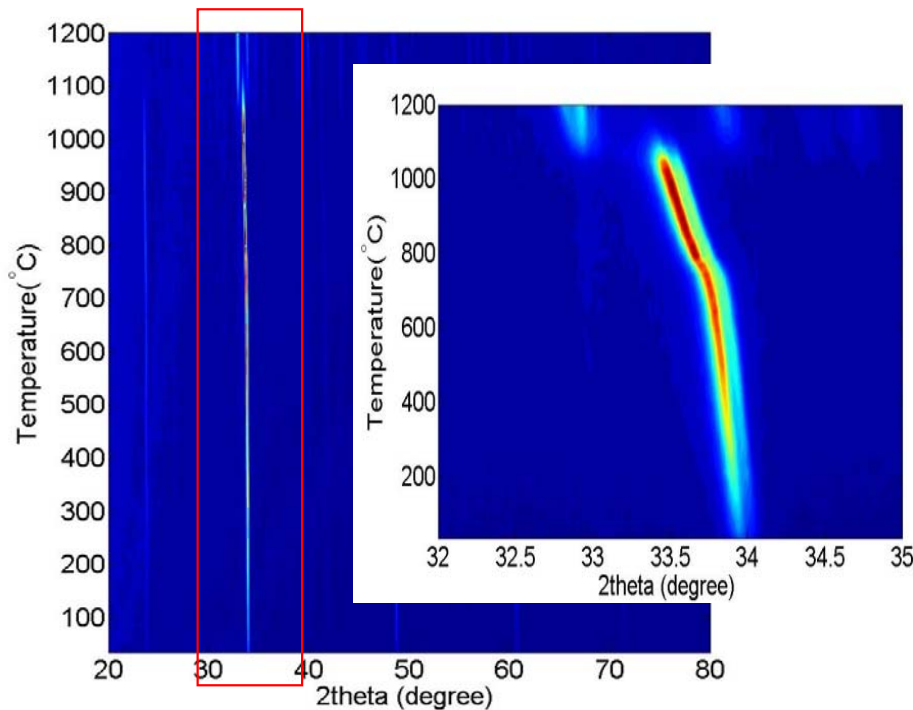
Stability Challenges for CaMnO₃



CaMnO₃ is chosen as the base material due to its well-known CLOU Properties

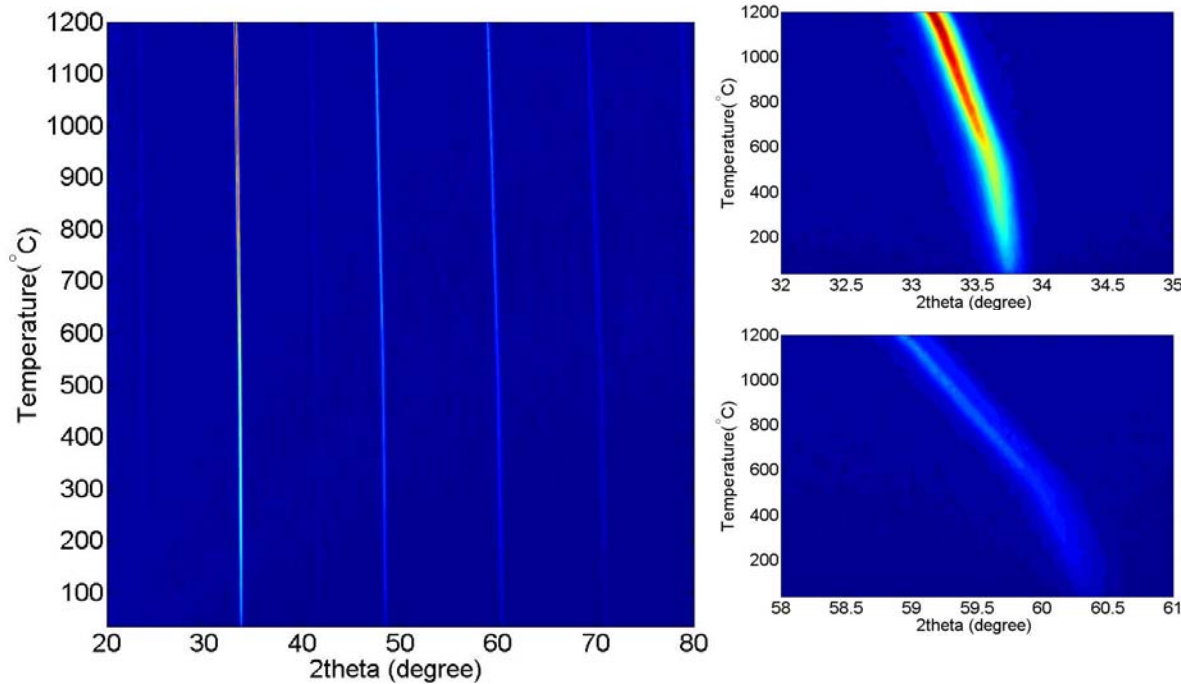
- Peaks begin to significantly shift between 800-850°C ; sign of oxygen uncoupling
- Up to 1100°C cubic CaMnO_{3-δ} remains stable

Stability of CaMnO_3 : *In-Situ* XRD Studies



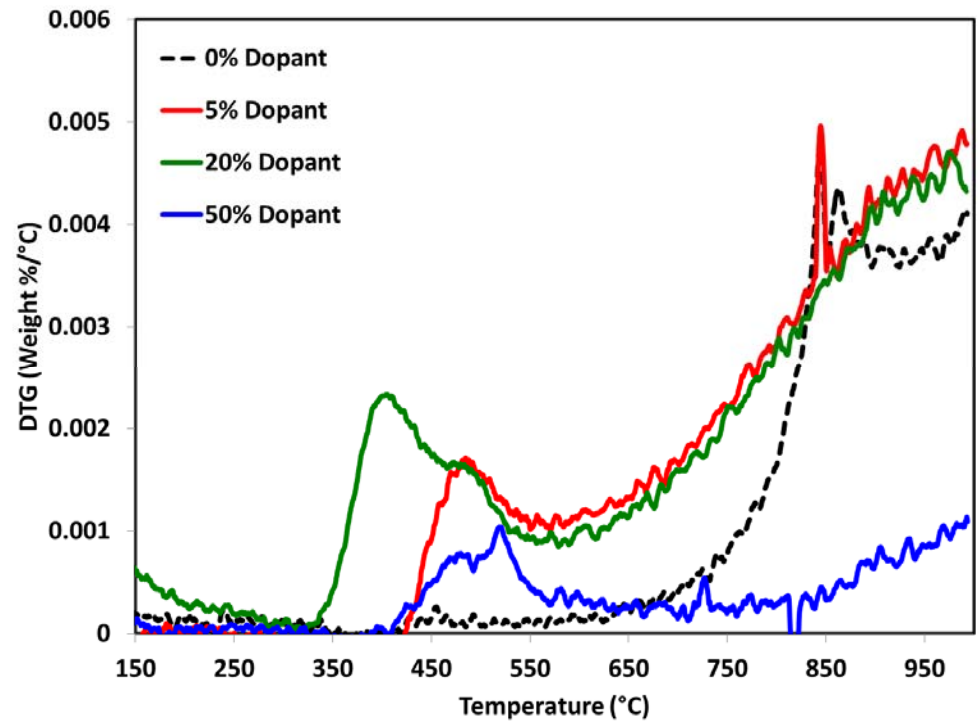
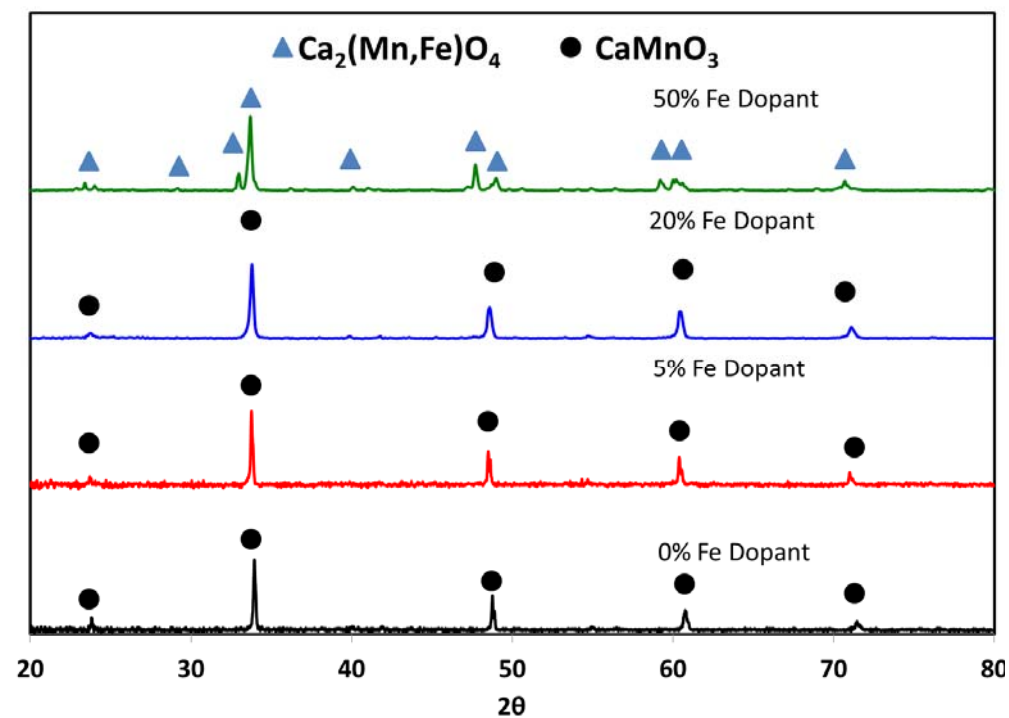
- After 1,100 $^{\circ}\text{C}$ spinel CaMn_2O_4 and Ruddlesdon-Popper Ca_2MnO_4 phases form
- *Irreversible phase transition also observed under isothermal cyclic conditions at lower temperatures*

Effect of Sr Substitution for CaMnO_3



No irreversible phase transition observed; significantly lowered uncoupling temperature

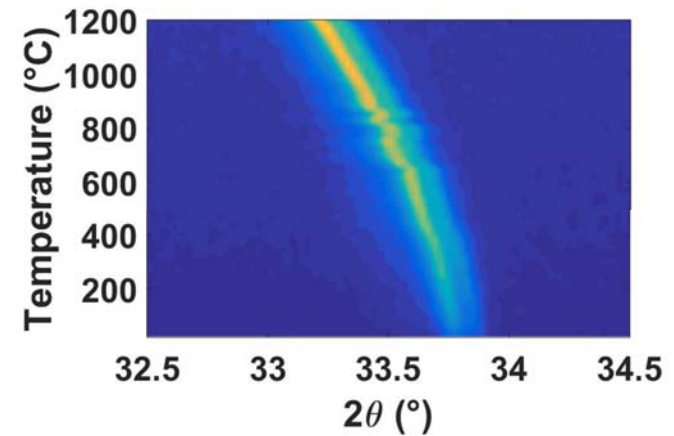
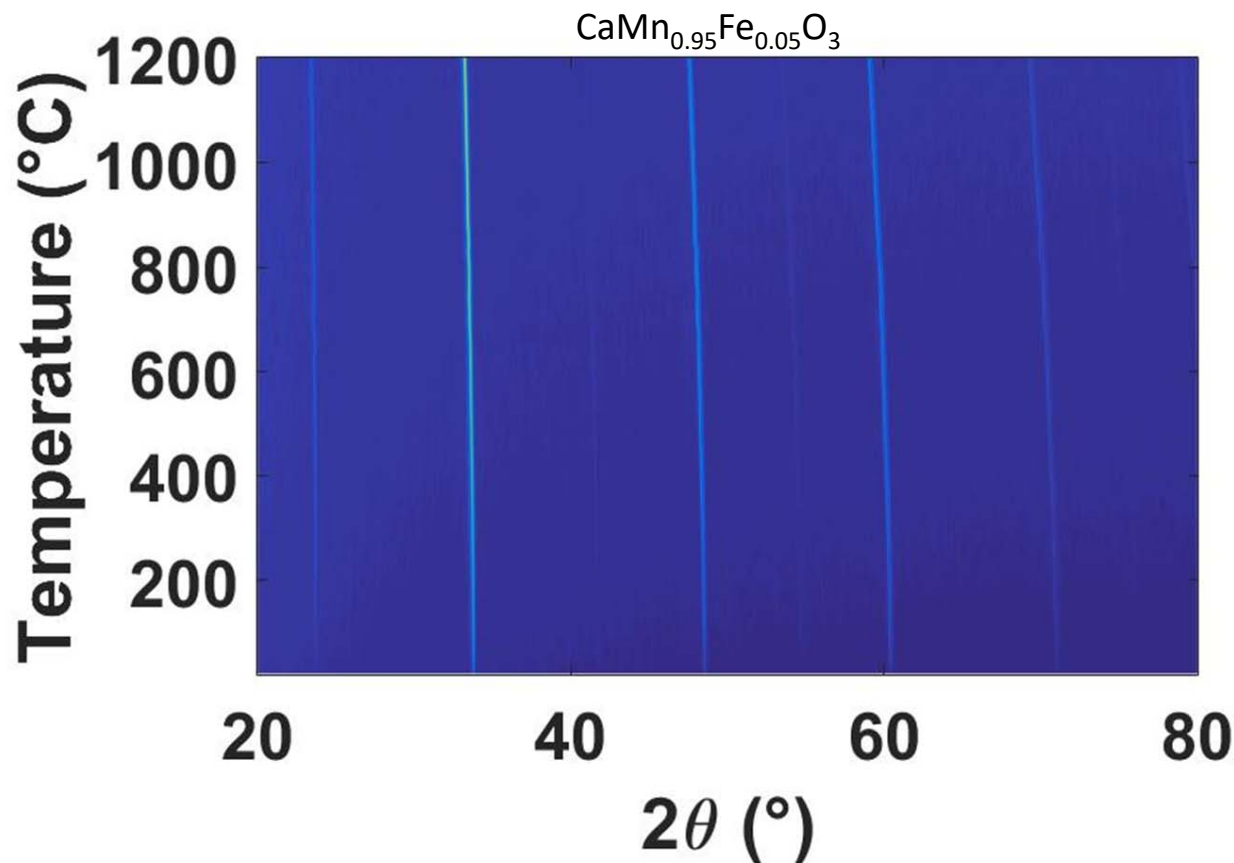
Effect of B-site Substitution for CaMnO_3 - Iron



Substitution of Fe into the B-site

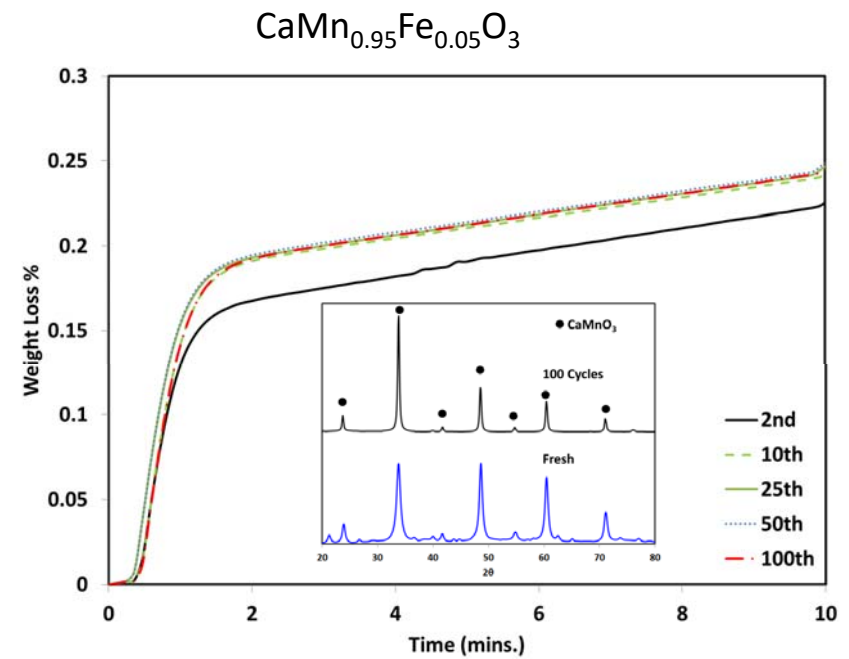
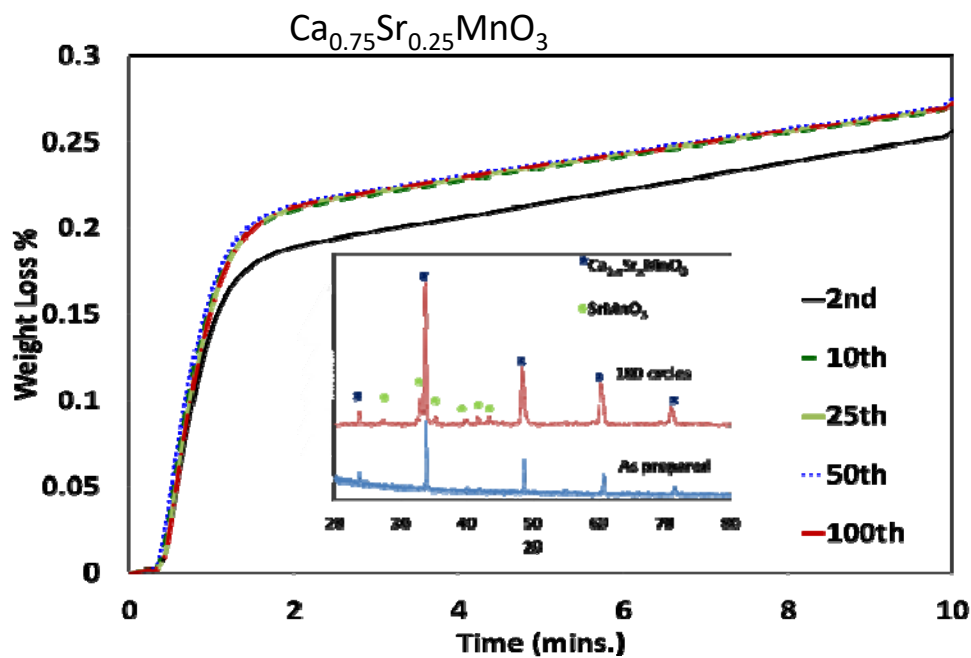
- Formation of solid solution at low Fe concentrations
- High Fe concentration induces a Ruddlesden-Popper phase
- α -oxygen release at low temperatures

Effect of B-site Substitution for CaMnO_3 - Iron



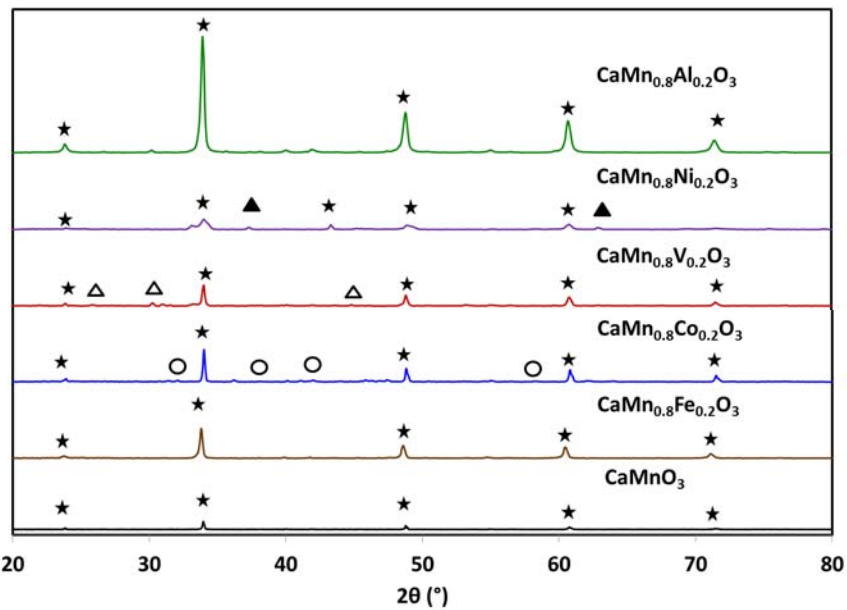
No irreversible phase transition
observed up to 1200 °C

Isothermal Cycles- Long Term Cycling

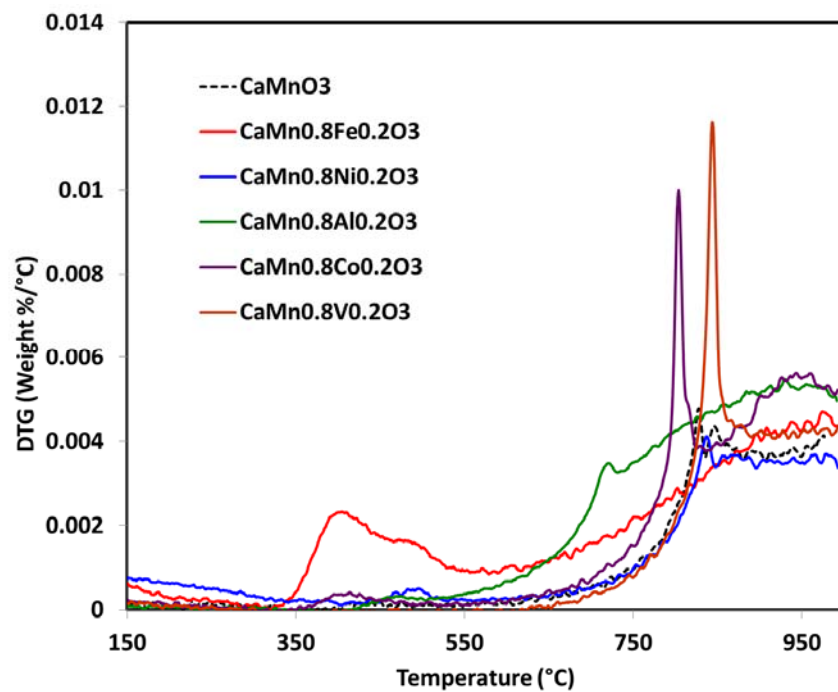


Substituted oxygen carriers are both redox stable for 100+ cycles. No undesirable phase transitions are observed after cycling.

Effect of B-site Substitution for CaMnO_3

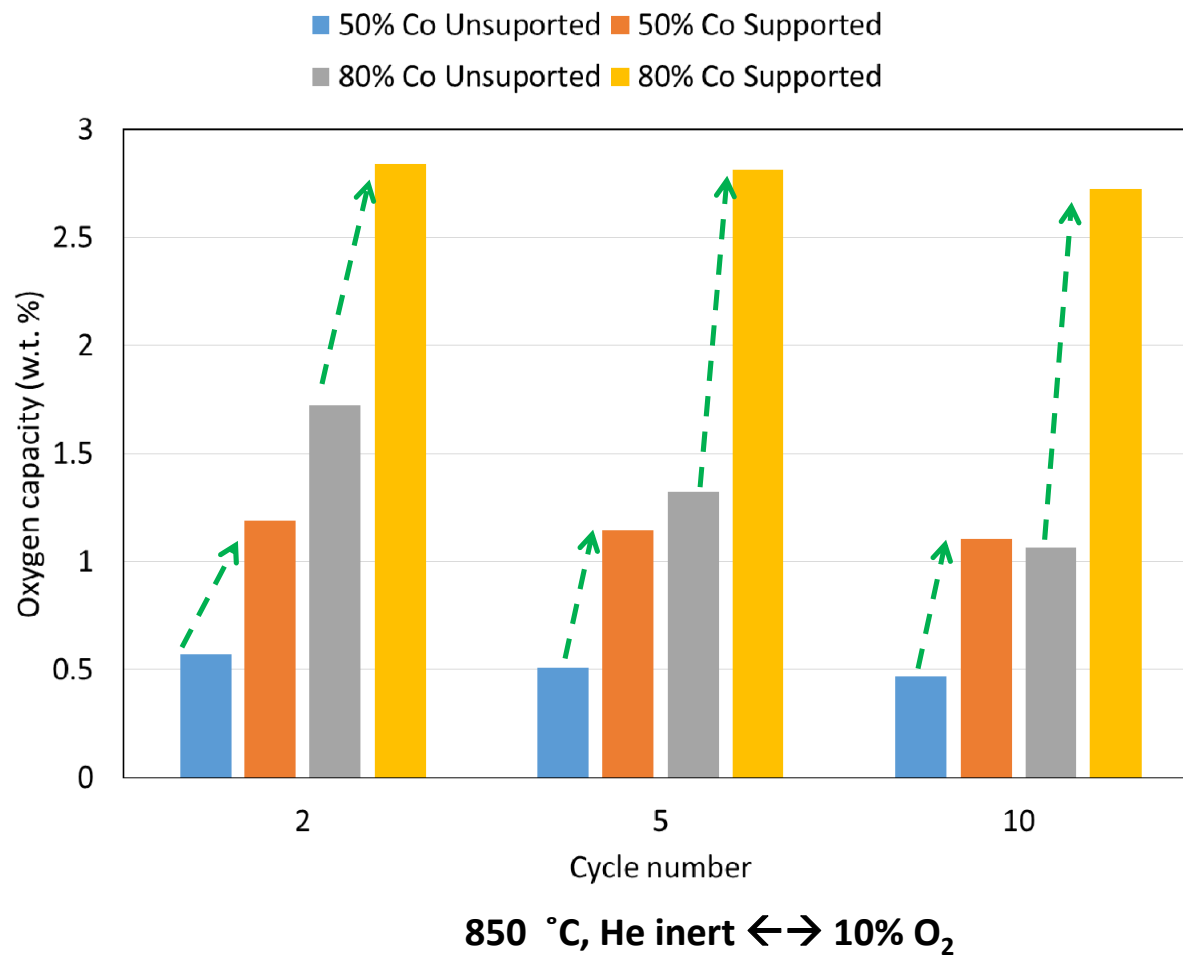


(★) CaMnO_3 (○) $\text{Ca}_3\text{Co}_{1.5}\text{Mn}_{0.5}\text{O}_6$ (Δ) V_2O_5 and (▲) NiO phases



B-site substitution also leads to oxygen carriers with varying oxygen release properties

Perovskite Supported Fe-Co and Fe-Mn CLOU Carriers



Up to 2.9 w.t.% oxygen carrying capacity achieved, supports significantly enhances the CLOU performance

Summary

- Char combustion is rate limiting for CLC, a desired P_{O_2} region could be developed for CLOU
- Vacancy formation energy can be an effective descriptor for oxygen carrier optimization
- DFT can provide valuable insights on oxygen carrier CLOU properties and phase stabilities
- A-site and B-site substitution in $CaMnO_3$ can enhance its redox stability and oxygen release properties
- Perovskite with good MIEC properties can also be effective as support for other oxygen-released mixed metal oxides

Journal Articles

- Nathan Galinsky and Fanxing Li "CaMn_{1-x}B_xO₃ (B=Al, V, Fe, Co, and Ni) Perovskite Based Oxygen Carriers for Chemical Looping with Oxygen Uncoupling (CLOU)" Applied Energy, 2016 174: 80-87.
- Amit Mishra, Nathan Galinsky, Feng He, Erik Santiso, and Fanxing Li "Perovskite-structured AMn_xB_{1-x}O₃ (A= Ca or Ba; B= Fe or Ni) redox catalysts for partial oxidation of methane." Catal. Sci. Technol., 2016 DOI: 10.1039/C5CY02186C.
- Nathan Galinsky, Arya Shafiefarhood, Yanguang Chen, Luke Neal, Fanxing Li "Effect of support on redox stability of iron oxide for chemical looping conversion of methane". Applied Catlaysis B: Environmental. 2015, 164: 371-379.
- Nathan Galinsky, Amit Mishra, Jia Zhang, and Fanxing Li* "Ca_{1-x}A_xMnO₃ (A= Sr and Ba) Perovskite Based Oxygen Carriers for Chemical Looping with Oxygen Uncoupling (CLOU)". Applied Energy, 2015 DOI:10.1016/j.apenergy.2015.04.020
- Arya Shafiefarhood, Amy Stewart, Fanxing Li* "Iron-Containing Mixed-Oxide Composites as Oxygen Carriers for Chemical Looping with Oxygen Uncoupling (CLOU)". Fuel. 2015, 139: 1-10
- Mishra A, Santiso E, Li F. "Screening of AMnO₃ perovskites for chemical looping with oxygen uncoupling (CLOU) through first principles calculations of oxygen vacancy formation energy." (in preparation)

Conference Presentations

- Fanxing Li, Manganese-Containing Oxides as Versatile Oxygen Carrying Agents for Chemical Looping Applications, 4th International Conference on Chemical Looping, September, 2016.
- Fanxing Li, Rational Design of Redox Catalysts for Hydrocarbon Oxidation, Water-Splitting and CO₂ Utilization, ACS 2016 Annual Meeting, August, 2016.
- Amit Mishra, Erik Santiso, Fanxing Li, Investigation of AxA'1-xMnyB1-yO3- δ for chemical looping with oxygen uncoupling (CLOU) through first principles calculations , ACS 2016 Annual Meeting, August, 2016.
- Arya Shafiefarhood, Nathan Galinsky, and Fanxing Li. "Mixed-oxides for carbonaceous fuel conversion with integrated CO₂ capture via chemical looping with oxygen uncoupling (CLOU)" 248th ACS National Meeting. San Francisco, CA. August 2014.
- Arya Shafiefarhood, Nathan Galinsky, Amit Mishra, and Fanxing Li. "Composite mixed oxides for chemical looping with oxygen uncoupling." 3rd International Conference on Chemical Looping. Gothenburg, Sweden. 10 September 2014. Conference Presentation.
- Nathan Galinsky, Amit Mishra, and Fanxing Li. "Perovskite Based Oxygen Carriers for Chemical Looping with Oxygen Uncoupling." 2014 AIChE Annual Meeting. Atlanta, GA. 19 November 2014.
- Mishra A, Santiso E, Li F. Perovskite Structured Redox Catalysts for Methane Partial Oxidation Using Lattice Oxygen. 2015 ACS, Boston, MS.

Acknowledgement

- Prof. Erik Santiso (Co-PI)
- Graduate Students:
 - Amit Mishra
 - Nathan Galinsky
 - Arya Shafiefarhood
- Undergraduate Students:
 - Lindsay Bowers
 - Grant Thomas
 - Rory Bergen
- Funding:
 - US DOE FE001247
- Project Managers
 - Jason Hissam and David Lyons



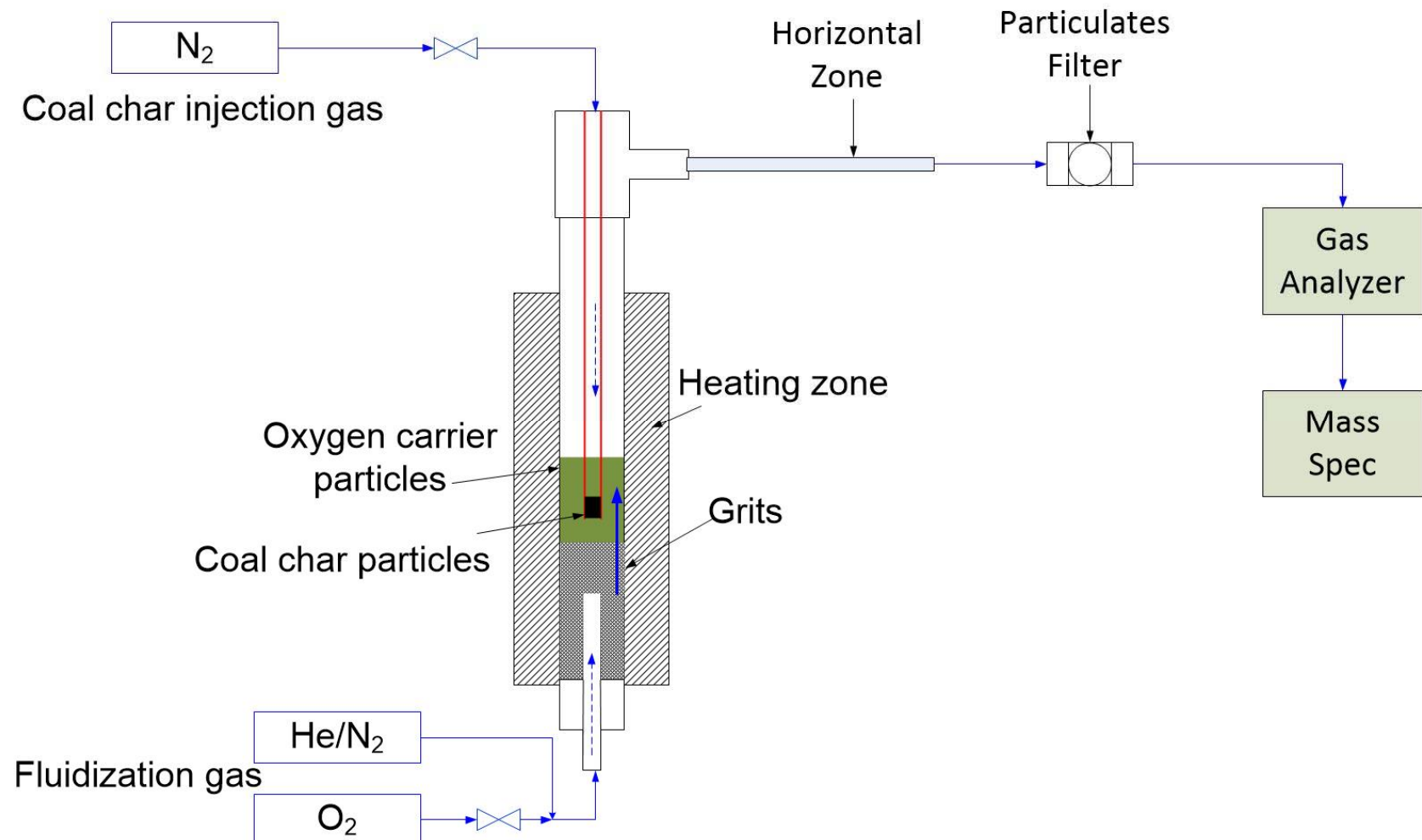
Thanks!



NC STATE UNIVERSITY

Supplemental Slides

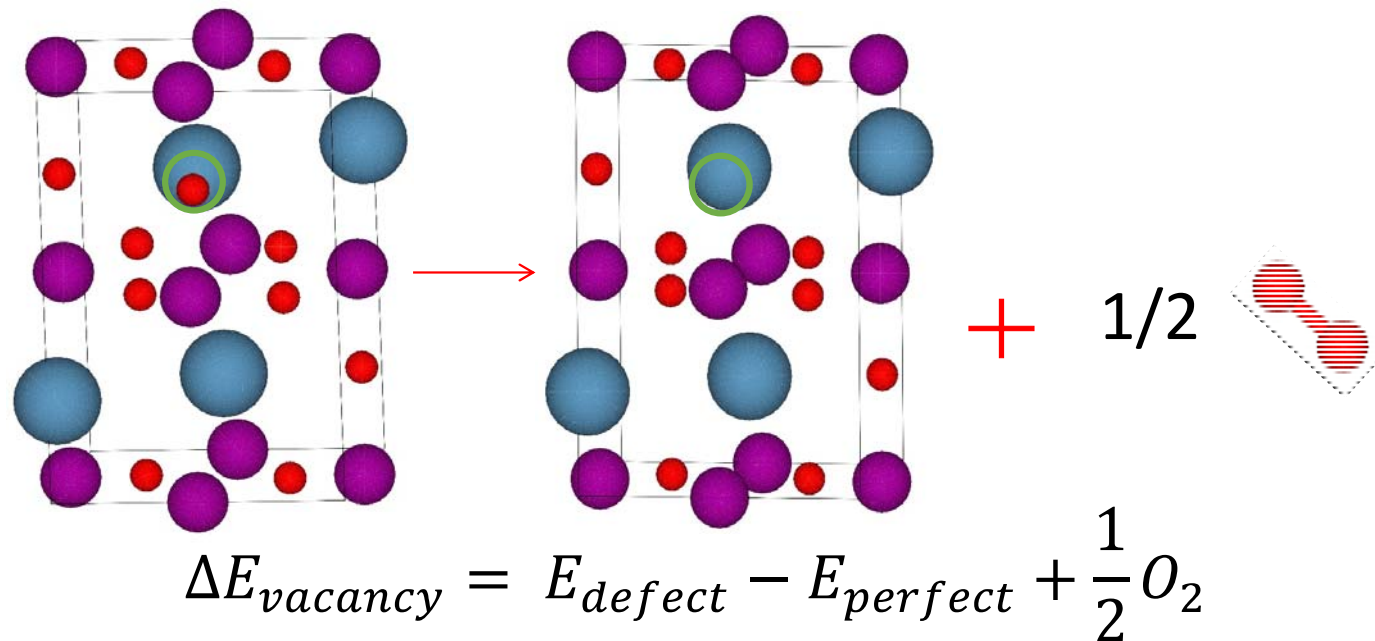
Fluidized Bed Setup



Proposed Approach

- Vacancy formation energy can provide thermodynamic basis for estimating CLOU capabilities
- DFT can provide such information via first principle calculations

Question: how to perform accurate yet efficient calculations?

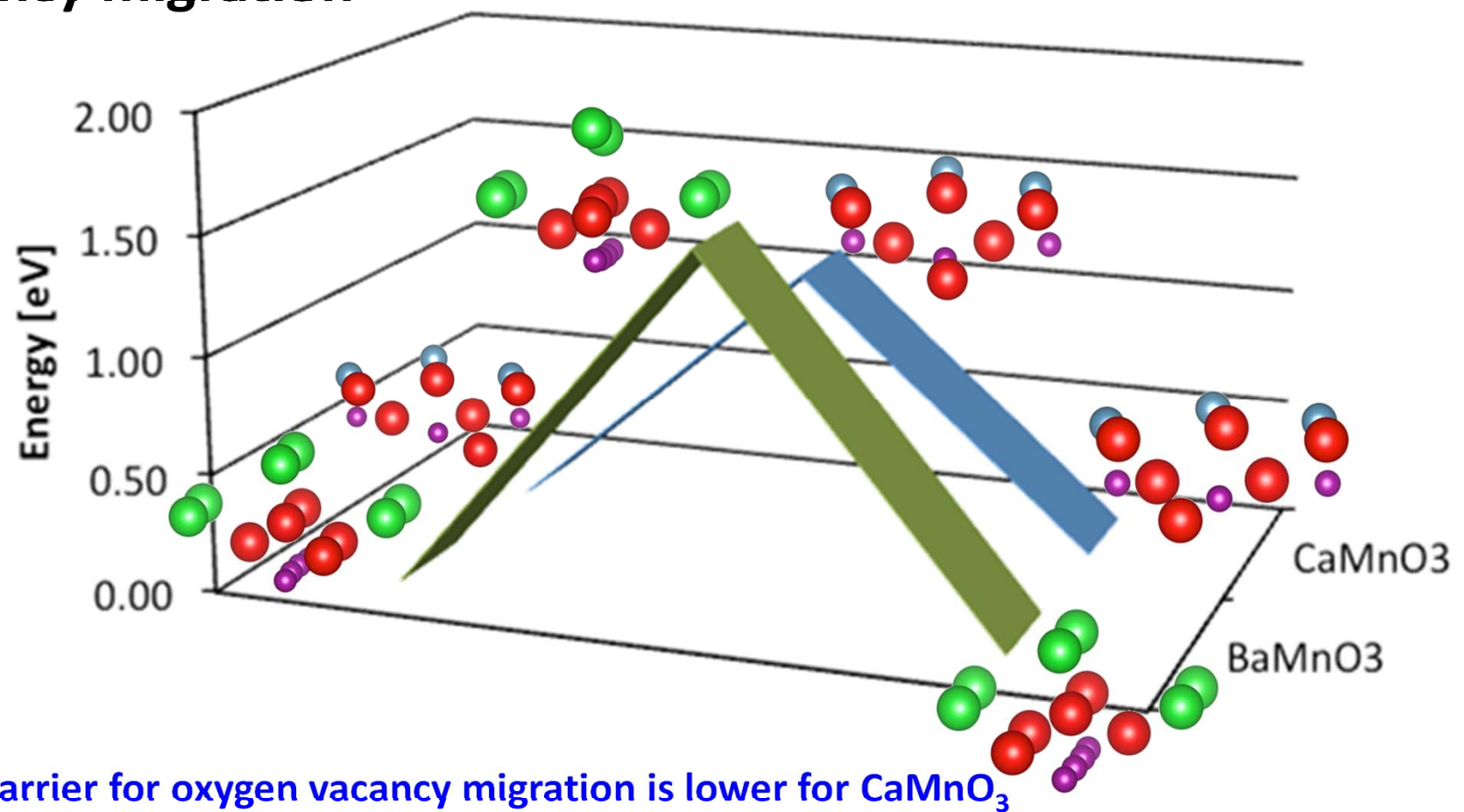


Simulation Strategy

- Practical considerations for efficient DFT screening:
 - Validity of DFT without U
 - Magnetic state considerations
 - Validity of neutral vacancy assumption
 - Vacancy formation energy at dilute limit
- Determination of screening methods:
 - DFT v.s. DFT+U
 - Formation energies for different charge states
 - CaMnO_3 and BaMnO_3 as model compounds

$$\Delta E_{vacancy} = E_{defect}^q - E_{perfect} + \frac{1}{2} O_2 + q(E_F + E_{VBM})$$

Preliminary Results: Climbing Image NEB of E_{barrier} for oxygen vacancy migration



DFT Parameters

VASP package

Electron Ion Interaction: PAW

Exchange correlation functional: PBE-GGA

Energy cut-off: 425 eV

EDIFF = 10^{-4} eV

Fixed mesh density for varying super cell sizes:

Orthorhombic CaMnO₃: 4x4x4 for 1 unit cell; monkhorst pack

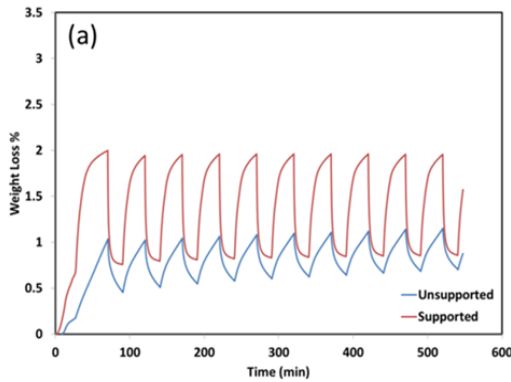
Orthorhombic Ca.75Sr.25MnO₃: 4x4x4 for 1 unit cell; monkhorst pack

Hexagonal BaMnO₃: 4x4x4 for 1 unit cell; Gamma centered

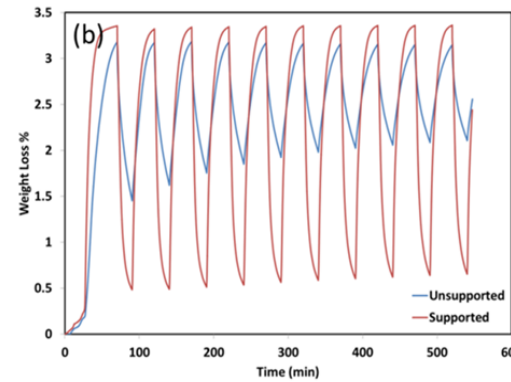
$$E_{O_V} = E_{AMnO_{3-\delta}} + \frac{1}{2}E_{O_2} - E_{AMnO_3}$$

Isothermal CLOU Testing ($850\text{ }^{\circ}\text{C}$, He inert \leftrightarrow 10% O_2)

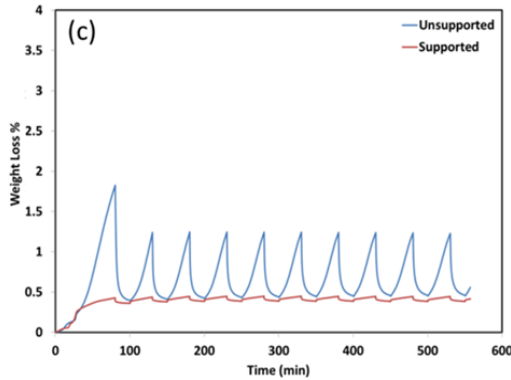
50% Co – 50% Fe



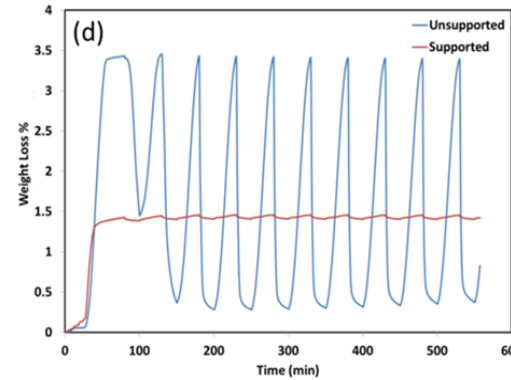
80% Co – 20% Fe



30% Mn – 70% Fe

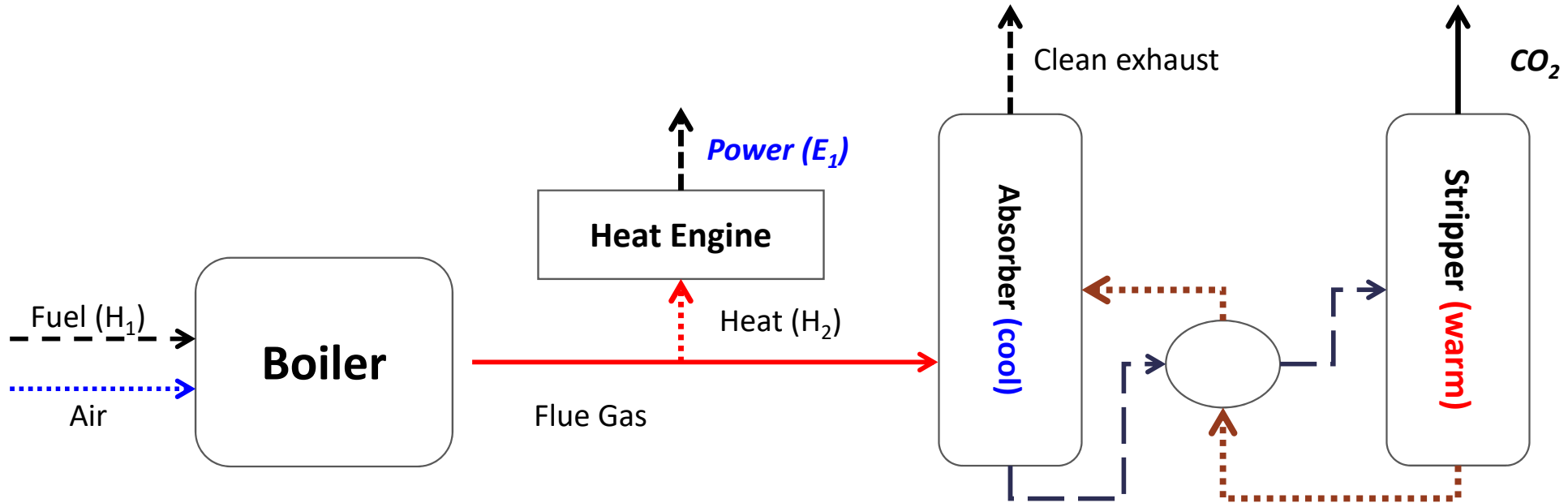


60% Mn – 40% Fe



- *CLOU properties of mixed Fe-Co oxides are enhanced by perovskite addition*
- *Oxygen carrying capacity of mixed Fe-Mn oxides under an isothermal condition is negatively affected by perovskite addition*

Why Chemical Looping: Conventional Post-Combustion CO₂ Capture

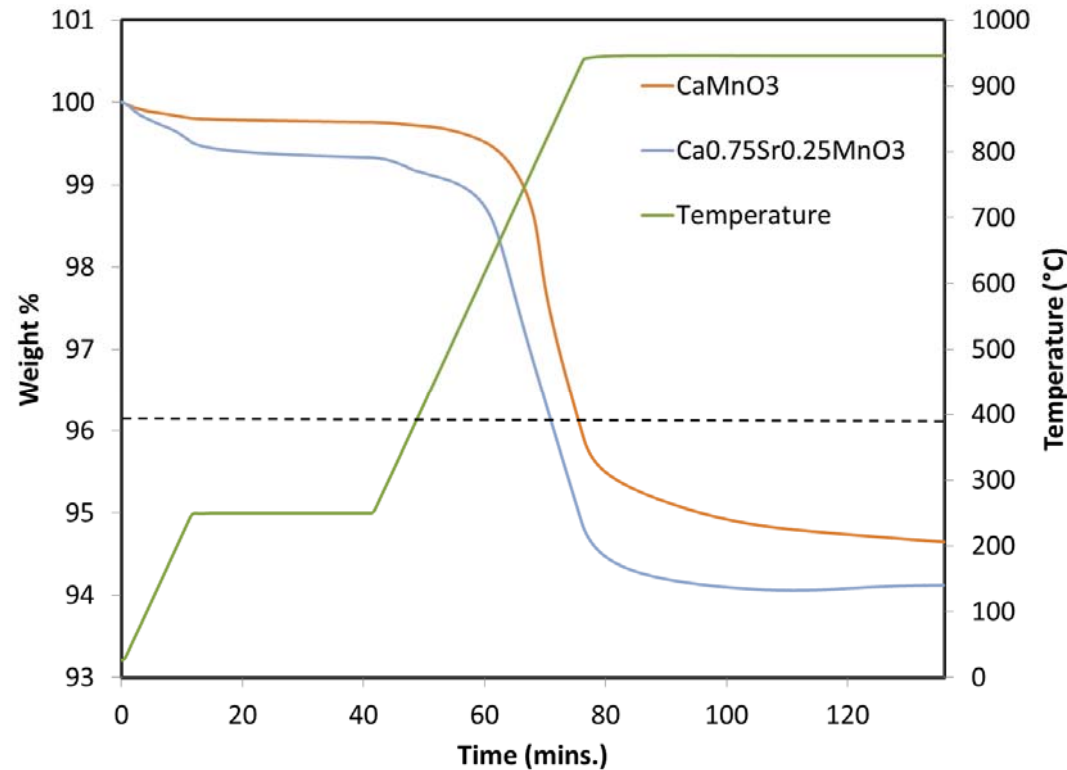


Limitations to conventional combustion – absorption based processes:

- Fixed extractable enthalpy from boiler/flue gas
- Absorber-stripper cycle consumes high grade heat and rejects low grade heat
- Delivery pressure of CO₂ is limited

Low 2nd Law efficiency!

Char Oxidation using Perovskites

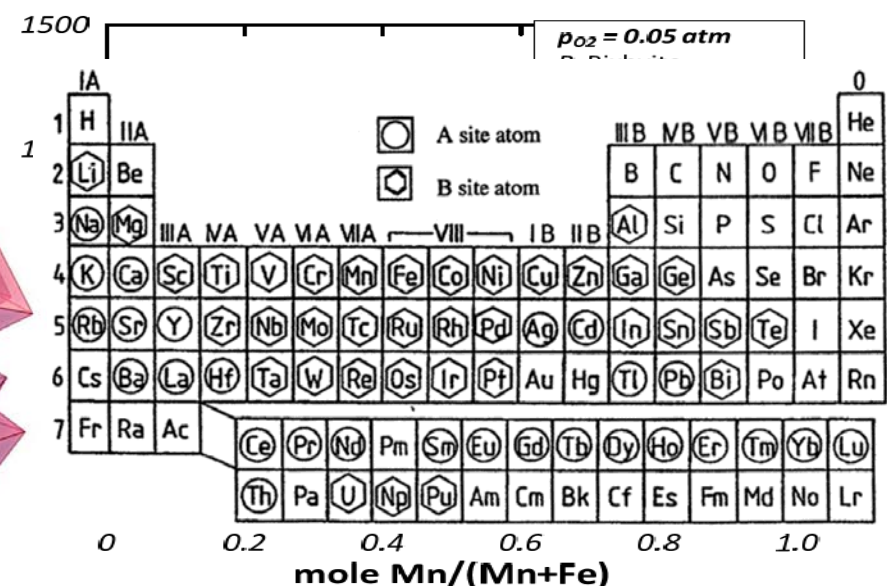
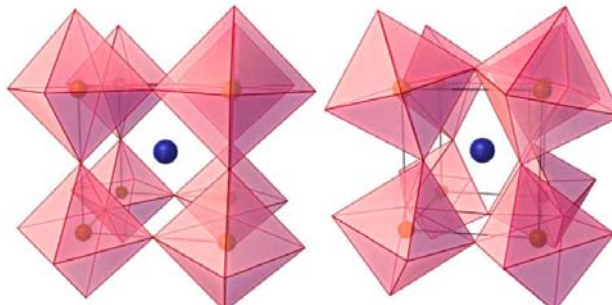


Sr doped perovskite shows notably lower reaction temperatures for char oxidation

Material Selection – Rapidly Expanding Material Design Space

oxygen carrier material selections

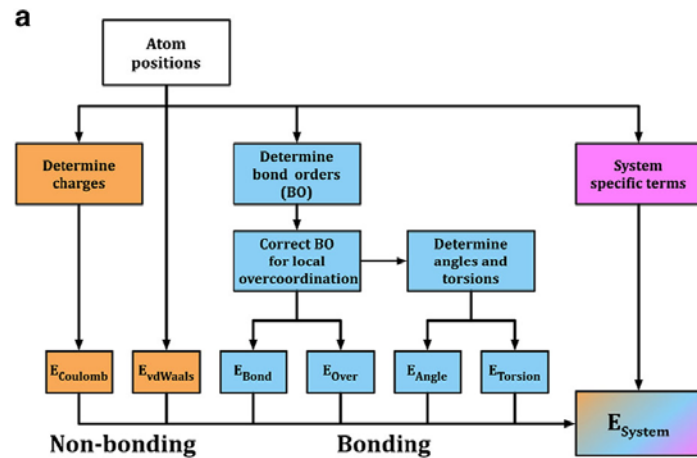
- Iron
- Copper
- Manganese
- Nickel
- Cobalt
- Perovskite materials
- Mixed first row transition metal oxides



M. Rydén et al., 2nd International Conference on Chemical Looping, 2012
Structure and Properties of Perovskite Oxides, Tatsumi Ishihara

Reactive force field (ReaxFF)

- ReaxFF is a continuous bond order force field
- Force field parameters are developed by fitting to electronic structure calculations for the system of interest.

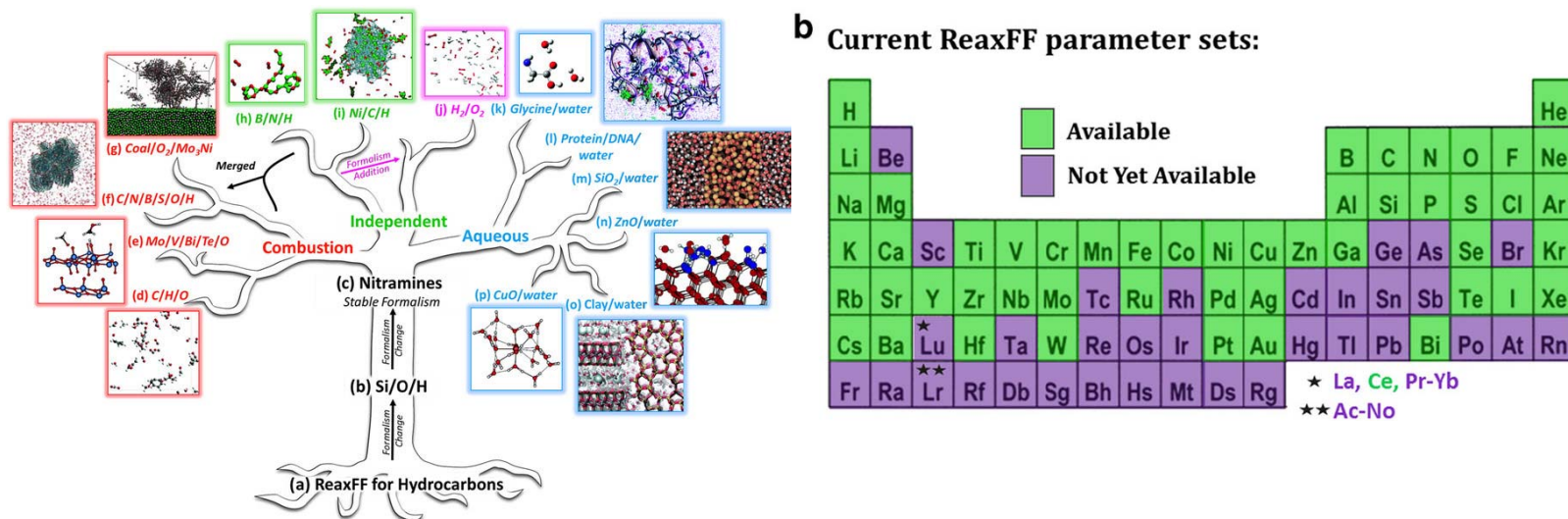


$$E_{\text{system}} = E_{\text{bond}} + E_{\text{over}} + E_{\text{angle}} + E_{\text{tors}} + E_{\text{vdWaals}} + E_{\text{coulomb}} + E_{\text{specific}}$$

$$BO'_{ij} = BO_{ij}^{\sigma} + BO_{ij}^{\pi} + BO_{ij}^{\pi\pi} = \exp \left[p_{bo1} \cdot \left(\frac{r_{ij}}{r_o^{\sigma}} \right)^{p_{bo2}} \right] + \exp \left[p_{bo3} \cdot \left(\frac{r_{ij}}{r_o^{\pi}} \right)^{p_{bo4}} \right] + \exp \left[p_{bo5} \cdot \left(\frac{r_{ij}}{r_o^{\pi\pi}} \right)^{p_{bo6}} \right]$$

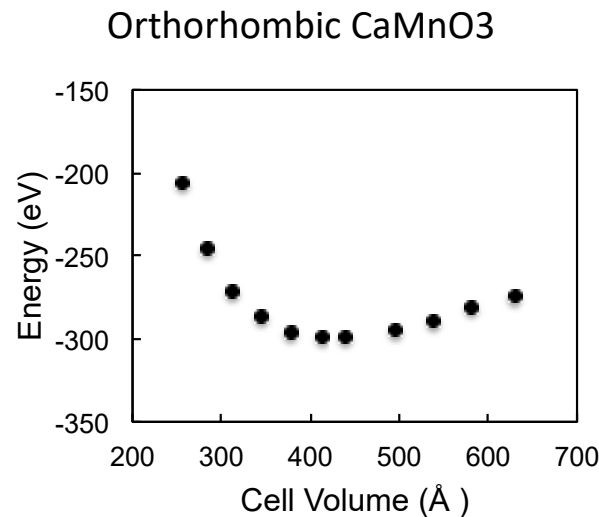
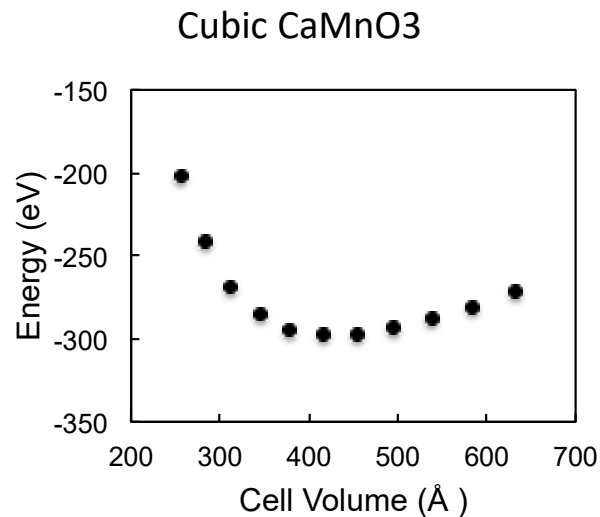
Reactive force field (ReaxFF)

- ReaxFF is a continuous bond order force field
- ReaxFF has been applied to a wide variety of applications
- Force field parameters are dependent on the systems used to fit them
- Parameters do not exist for all combinations of atoms



Building a training set for CaMnO_3

Crystal ‘phase diagrams’ from DFT calculations



Still in progress ...